2019

# THE ORIGIN OF AN ARCHEAN BATHOLITH IN MICHIGAN'S UPPER PENINSULA

Brandi Petryk

# THE ORIGIN OF AN ARCHEAN BATHOLITH IN MICHIGAN'S UPPER PENINSULA

By

Brandi Michelle Petryk

A THESIS

Submitted in partial fulfillment of the requirements for the degree of

MASTER OF SCIENCE

In Geology

MICHIGAN TECHNOLOGICAL UNIVERSITY

2019

This thesis has been approved in partial fulfillment of the requirements for the Degree of MASTER OF SCIENCE in Geology.

Department of Geological and Mining Engineering and Sciences

Thesis Advisor: *Dr. Chad Deering*

Committee Member: *Dr. Theodore Bornhorst*

Committee Member: *Dr. Olivier Bachmann*

Department Chair *Dr. John Gierke*

Table of Contents

# List of figures

# List of tables

# Acknowledgements

I would like to express my thanks to Dr. Chad Deering for guidance and support during this research. I would also like to thank the Geology department at Michigan Tech, everyone was so welcoming and helpful throughout my two years here. A huge thank you to my family and friends for their constant love and support. Thank you to Bob Barron and Anthony Deciechi for the extraordinary help in the field and the lab, you guys rock! Thank you to Olivia Barbee for your guidance and lab training, you're an inspiration.

This work was partially funded by the Michigan Space Grant Consortium, NASA grant #NNX15AJ20H, for without this support my research would not have been completed.

# Abstract

The Southern Complex is part of the Archean Superior Province in the Upper Peninsula of Michigan and includes a batholithic sized body of Archean high-K megacrystic granitoid rocks informally called the Bell Creek granite. U-Pb zircon ages of the granitoid from previous studies suggest an emplacement age of ~2.6 Ga (Tinkham, 1997). Based on those ages the Bell Creek granite formed around the Archean-Proterozoic transition. This transition is a crucial time period in Earth's history for crustal growth because of the onset of subduction and increased sedimentary environments at the end of the Archean (Taylor and McLennan, 1995). In this study we tested two models hypothesized for the origin of granitoids. The first model involves juvenile magma from the mantle that undergoes differentiation and the remaining silica-rich melt separates, ascends and cools to form a granitoid; may include assimilation of country rock. The second model involves the partial melting of preexisting lower crustal basement lithologies; may include assimilation of country rock. To test the two models a combination of U-Pb and O-Hf isotopes was employed, in addition to petrological observations. The results of the U-Pb zircon dating suggests a 2.5-2.6 Ga emplacement age for the Bell Creek granite. Inherited zircons range in age from 2.7-4.2 Ga, suggesting that supracrustal material of various ages contributed to the overall petrogenesis of the Bell Creek granite. The $\delta^{18}O$ (VSMOW) values of the zircons ranges from +5.0 to +13.0‰, representing a range from mantle (+5.5‰, Valley, 2005), to crustal values (>8.0‰, Valley, 2005). The εHf(t) values range from -20 to -5, and yield a Hf model age of approximately 3.3 Ga, signifying isotopic ingrowth. The high-K nature of the granites suggests that a pelitic

material was assimilated during petrogenesis; the range in $\delta^{18}O$ values of the zircons with magmatic U-Pb ages is evidence that supports this hypothesis. Hoffman (1987) suggested that the Bell Creek was emplaced in a suite of metasedimentary and metavolcanics rocks, this could be the source of the assimilated pelitic material. Remnants of pelitic material are present in the high-K granites as biotite-chlorite-garnet dominated clots. Hoffman (1987) concluded that the Bell Creek granite is an S-type granite and a product of partial melting of sediments. However, magmatic zircons with mantle-like $\delta^{18}O$ values supported by bulk-rock major and trace elements suggest the Bell Creek granite is an I-type. The $\delta^{18}O$ isotopic results supports partial melting and assimilation of sedimentary material which is consistent with Hoffman's (1987) previous conclusion of assimilation. Comparison of the emplacement age of the Bell Creek (2.55 Ga) and the Hf model age (3.3 Ga) supports a hypothesis that the Bell Creek granite is a product of partial melting of a possible amphibolite source rock that was produced 1 Ga prior to emplacement of the granite.

# 1 Introduction

The Archean eon encompasses a third of geological history on our planet and during this time the majority of continental crust is thought to have formed (Sylvester, 1994; Taylor & McLennan, 1985; Choukroune et al., 1997). The Archean had a higher heat flow than post-Archean eons and, as a consequence, this promoted the subduction of young hot oceanic lithosphere and a concomitant increase in growth rate of continental crust (Taylor, 1987; Taylor & McLennan, 1995; Choukroune et al., 1997). The subducted material partially melted and led to the production of low-K tonalite-trondhjemite-granodiorite suites (TTG; Jahn et al. 1981). The early Archean crust is interpreted to consist of bimodal lithologies: the TTG suites and granite-greenstone belts (Sylvester, 1994; Taylor & McLennan, 1995). Granite-greenstone belts are comprised of metamorphosed mafic/ultramafic volcanic rocks and associated sedimentary rocks that are intruded by granites and often associated with convergent plate boundaries (Kusky, 1999). Near the end of the Archean large scale intracrustal melting of newly formed crust lead to the production of K-rich granitoids and granites that dominated the upper crust (Sylvester, 1994; Taylor & McLennan, 1995: Choukroune et al., 1997). High-K granitoids are a known constituent of late Archean cratons and typically intrude the low-K granitoid gneisses of the TTG suites. High-K granitoids, in particular, have been interpreted to be a product of partial melting of preexisting continental material (Sylvester, 1994; Moyen et al., 2003; Kumar et al., 2011; Laurent et al., 2014).

The Superior Province is the largest Archean craton representing the core of the Canadian shield and, therefore, may provide important clues for understanding late Archean crustal growth (Card, 1986; Corfu, 1988; Choukroune et al., 1997). This study focuses on the origin of an Archean batholith in the Southern Complex within the Superior Province (Figure 1). The age and origin of this complex has been debated for years and still is uncertain. It was originally thought to be genetically related to similar lithologies found in the nearby Northern Complex (Cannon and Simmons, 1973; Van Schmus and Woolsey, 1975). However, the Southern Complex is separated from the Northern complex by the Great Lakes Tectonic Zone (GLTZ), which is a continental scale suture/fault zone (Morey and Sims, 1976; Sims et al., 1980). Tinkham (1997) determined an emplacement of the granitoids of the Southern Complex at ~2.61 Ga using U-Pb dating on zircon. An age of ~2.61 Ga would place the magmatic age of the Southern Complex at the end of the Archean during the Archean-Proterozoic transition. The Archean-Proterozoic transition also marked a shift from the production of dominantly mantle-derived magmas that differentiated to form new continental crust to the first stages of significant recycling of crustal material (Taylor & McLennan, 1995; Valley, 2005). This is a crucial time period in Earth's history due to a decrease in global heat flow, the onset of 'modern-day' subduction and an increased number of sedimentary environments (Taylor, 1987; Taylor and McLennan, 1995). During this period major tectonic stabilization was occurring as stable cratons formed by massive intra-crustal melting to produce granitoids via devolatilization (Pollack 1986; Taylor & McLennan, 1995). Hoffman (1987) suggested that the granitoids in the Southern Complex are S-type, having been produced by partial melting of metasedimentary and/or

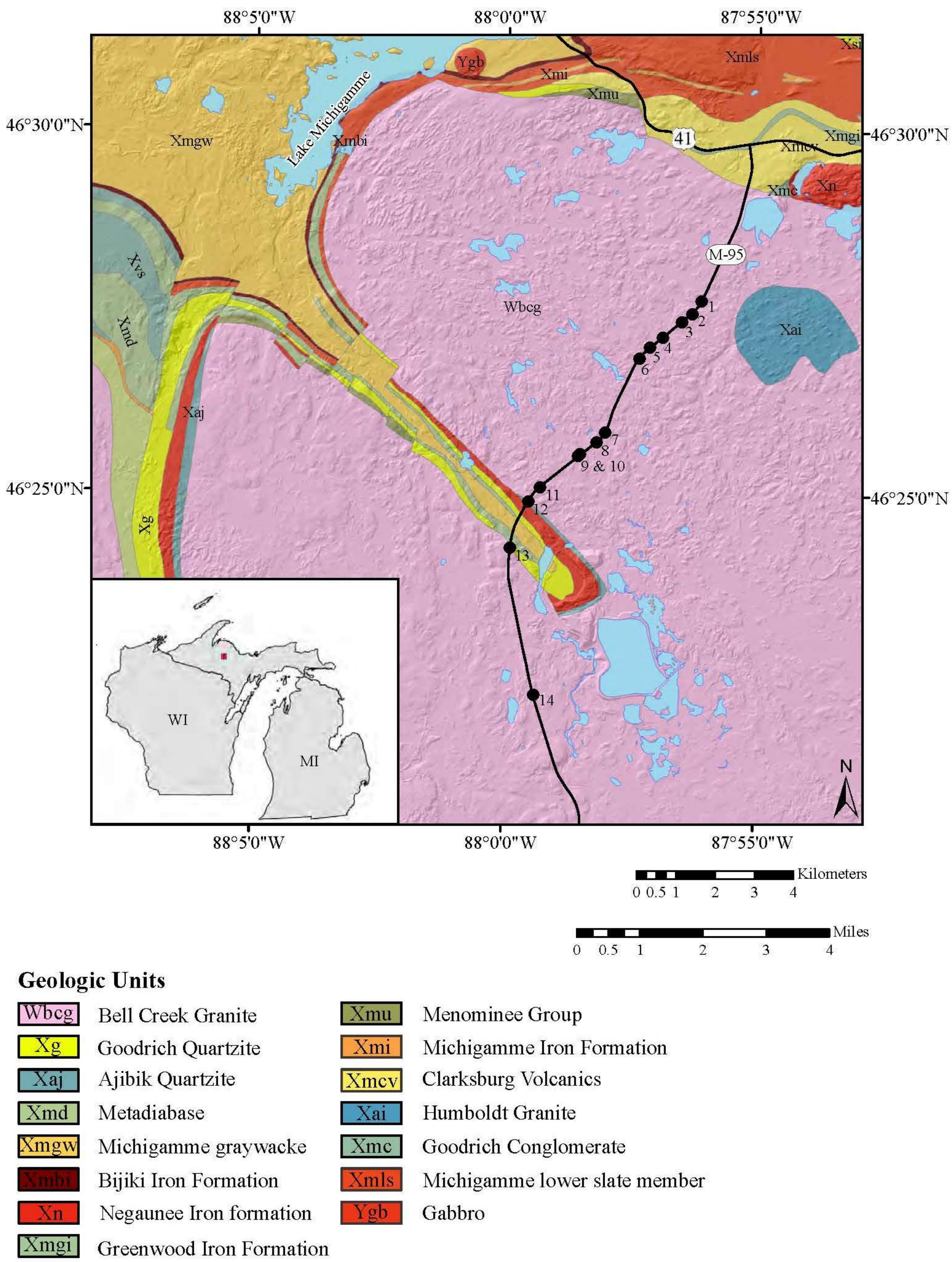


**Figure 1** Geologic map of the Southern Complex corridor M95 with rock sample locations, modified from Cannon and Simmons (1973).

amphibolitic basement rocks that later assimilated sediments as the magma rose through the crust.

Generally, there are two hypothesized models for the origin of granitoids: 1) Juvenile magma from the mantle undergoes differentiation, and the remaining silica-rich melt separates, ascends, and ultimately cools to form a granitoid; or 2) Preexisting lower crustal basement lithologies undergoes partial melting and possible assimilation of country rock which can result in the formation of a granitoid (Atherton, 1993; Pitcher, 1993; Brown, 1994, 2007; Taylor and McLennan, 1995). One of the most effective ways to evaluate the models of crustal evolution is to integrate geochronological, geochemical and petrological data. Zircon has been extensively studied and is known to give reliable ages and estimates for host rock genesis and protolith composition (Valley, 2003). Zircon is among one of the most common accessory minerals in igneous, sedimentary and metamorphic rocks (Finch & Hanchar, 2003) that also happens to have a high closure temperature (~900°C) and, therefore, locks in the isotopic ratio at the time of zircon saturation in the melt. This characteristic of zircon ensures that the original isotopic concentrations have a higher chance of withstanding subsequent periods of high-grade metamorphism and/or partial melting (Lee et al., 1997).

The use of both oxygen and hafnium isotopes in zircon has been shown to be particularly useful for determining whether or not a magma formed from melting of juvenile mantle or from partial melting of preexisting crust (Hawkesworth & Kemp, 2006; Matteini et al. 2010). Zircons have been found to preserve their $\delta^{18}O$ value at the time of magmatic crystallization (Valley, 2003). In general, mantle oxygen isotopes are typically low (~5.5‰ $\delta^{18}O$) as compared to crustal rocks which are higher (>8‰ $\delta^{18}O$) (Valley, 2003), thus any crustal contamination will yield a higher $\delta^{18}O$ value. Depleted mantle sources will trend towards a +εHf value and while a component with crustal contamination will trend towards a -εHf value (Kinny & Maas, 2003; Vervoort, 2014).

The Lu-Hf isotopic system can be used to determine a model age for extraction of the source rock from the mantle (Matteini et al. 2010). The Hf isotope ratio of the zircons provide a crustal residence time for the zircons since crystallization (Hawkesworth & Kemp, 2006). Combining the Hf model age with U-Pb zircon ages and O isotopes allows for modeling the origin, igneous activity and petrogenesis of the granite system (Hawkesworth & Kemp, 2006).

This study presents field observations combined with bulk-rock major and trace elements and new zircon U-Pb dates and O-Hf isotopic data for the Bell Creek granitoids in the Southern Complex. These data were combined to test the two general models of granitoid genesis for the Southern Complex.

# 2 Background

The Southern Complex is part of an Archean high-grade gneiss terrane that collided into the Superior province around 2.7 Ga along the GLTZ (Sims, 1991). The Southern Complex lies south of the GLTZ. The Southern Complex is comprised of mafic to granitic gneisses and migmatite intruded by granite (Figure 1; Cannon and Simmons, 1973; Hoffman, 1987). The Southern Complex was first subdivided into the Compeau Creek gneiss and the Bell Creek (granite and gneiss) (Gair and Thaden, 1968). The Compeau Creek gneiss was originally defined by Gair and Thaden (1968) as a gneissic complex in the Northern Complex and they correlated this unit to the Southern Complex due to similar lithologies and structure, however, subsequent recognition of the GLTZ invalidates this correlation. Hoffman (1987) abandoned the name of Compeau Creek gneiss for rocks in the Southern Complex.

Tinkham (1997) subdivided the Southern Complex into the Twin Lake Assemblage and the Bell Creek assemblage. Tinkham (1997) interpreted the Twin Lake Assemblage as representing the remnants of a 2.8 Ga Archean granite-greenstone terrane that was intruded by the 2.6 Ga Archean Bell Creek Assemblage during a major tectonothermal event.

The focus of this study is the 2.6 Ga Bell Creek assemblage of Tinkham (1997) that consists of coarse-grained, light pink to gray granites distinguished by porphyritic texture and 2-5cm megacrysts of microcline. The assemblage includes the Bell Creek gneiss that is similar in appearance to the granite but with compositional banding and aligned megacrysts (Tinkham, 1997). Hoffman's Bell Creek granite and gneissic complex are synonymous with Tinkham's Bell Creek assemblage. Hoffman further subdivides the Bell

Creek granite into six subgroups based on important variations in hand-specimen textures and mineralogies: 1) Normal Bell Creek granite, 2) Foliated Bell Creek granite, 3) Altered Bell Creek granite, 4) Equigranular Bell Creek granite, 5) Fine-grained Bell Creek granite, and 6) Probably Bell Creek granite. The granite samples in this study will be referred to by these subgroups.

# 3 Methods

In this study, rock samples were collected from road outcrops along the Northern stretch of highway M95 which were previously mapped by Hoffman (1987) (Figure 1). Samples were taken from all rock types at each outcrop and only the granitoids were selected for analysis. All rock sample preparation and zircon extraction were completed using Michigan Technological University's facilities. Fifteen representative samples of granitoids were selected for bulk rock analysis, thin section preparation and zircon extraction. Zircons were extracted by crushing the rock and wet sieving to 45µm-200µm in size. The sorted particles were density separated using a heavy liquid, methylene iodide, with a density of $3.3 g/cm^3$. The magnetic grains were separated using a Frantz Magnetic separator. Approximately 100 zircons from each representative rock sample were randomly hand-picked under a binocular microscope and mounted on a 2.5 cm diameter cylinder epoxy mount.

Whole rock chemical composition was determined by Activation Laboratories Ltd. Rock samples were crushed and mixed with a flux of lithium metaborate and lithium tetraborate and fused in an induction furnace. The major and trace elements were analyzed by Perkin Elmer Sciez ELAN 6000 inductively coupled mass spectrometry (ICP-MS), three blanks and five control samples were analyzed with each group of unknown samples and the instrument was recalibrated every 40 samples.

Oxygen isotope data was obtained on individual zircon grains at the WiscSIMS laboratory at the University of Wisconsin-Madison. Oxygen isotope analysis was completed prior to U-Pb and Hf analysis, to minimize the potential for isotope fractionation induced by laser ICP-MS. Only one of the two zircon mounts were analyzed for oxygen, rock samples with oxygen data are given in Appendix 1. To ensure sample flatness the zircon mount was sent to the WiscSIMS laboratory to evaluate the relief using an optical profilometer. During preparation, a selection of grains of KIM-5 zircon oxygen isotope standard were mounted in the center of the Bell Creek zircon mount. Prior to analysis zircons were imaged by a reflected light microscope. Backscattered electron (BSE) images were obtained using a Hitachi S-3400N Scanning Electron Microscope (SEM), both images were obtained from the University of Wisconsin-Madison. Maps created from reflected light and SEM images aided in selecting spot locations for the analysis of the zircons. The cores of the zircon grains were preferentially chosen to avoid metamorphic rims. Oxygen-isotope ratios were measured using a CAMECA IMS-1280 ion microprobe with a 10μm beam following the procedures described by Kita et al. (2009). All data were acquired during one 12-hr session. Four zircon standard KIM-5 analyses were performed at the beginning of each bracket of analyses, and following every 15 unknowns. The bracket average values of the standards and unknowns were calculated at the end of each group and were used to correct for instrumental bias. Oxygen isotope results that fell above a relative yield of 1.05 were excluded from the results.

The U-Pb data (Appendix 6) were collected at Eidgenössische Technische Hochschule (ETH) Zürich using a Resonetics Resolution S155 laser ablation system coupled to a Thermo Element XR Sector-field ICP-MS with a 20μm beam diameter. The operating parameters were the same as outlined by Guillong et al. (2014) and are given in Appendix

2, Table 1. Target analysis sites for U-Pb were the same as previous oxygen sites, if no previous oxygen analysis was done the zircon cores were preferentially targeted to try to identify igneous magmatic ages. Analyses that represented inherited cores, metamorphic growth rims or metamict zones, as noted by anomalously old or young $^{207}Pb/^{206}Pb$, were excluded from U-Pb concordia and mean age calculations (Appendix 8). Analyses that fell outside of the range of 85-105% concordance were also excluded from age calculation.

Hafnium analysis (Appendix 7) was conducted at ETH Zürich using a Resonetics Resolution S155 laser ablation system coupled to a NU Plasma II sector-field multi collector ICP-MS with a 50μm beam diameter. The operating parameters were the same as outlined by Galli et al. (2019) and are given in Appendix 2, Table 3. About 20 zircons from each rock sample were analyzed and the target site was on or next to U-Pb analyses locations depending on the amount of material available. Due to the increase of spot size with Hf, larger zircons were preferentially chosen for analysis.

# 4 Results

## 4.1 Petrography

The Bell Creek assemblage is composed mainly of granitoid rocks. It is coarse-grained and ranges in color from white-gray to pink-red. This unit is best recognized by microcline megacrysts that range in size from ~0.5cm to ~5cm and can be white or light salmon in color (Figure 2). The microcline megacrysts in most samples define a fabric with alignment of their long axes (Figure 2b; *detailed descriptions can be found in Appendix 12*). The Bell Creek granitoid has an estimated mineral assemblage that consists of quartz

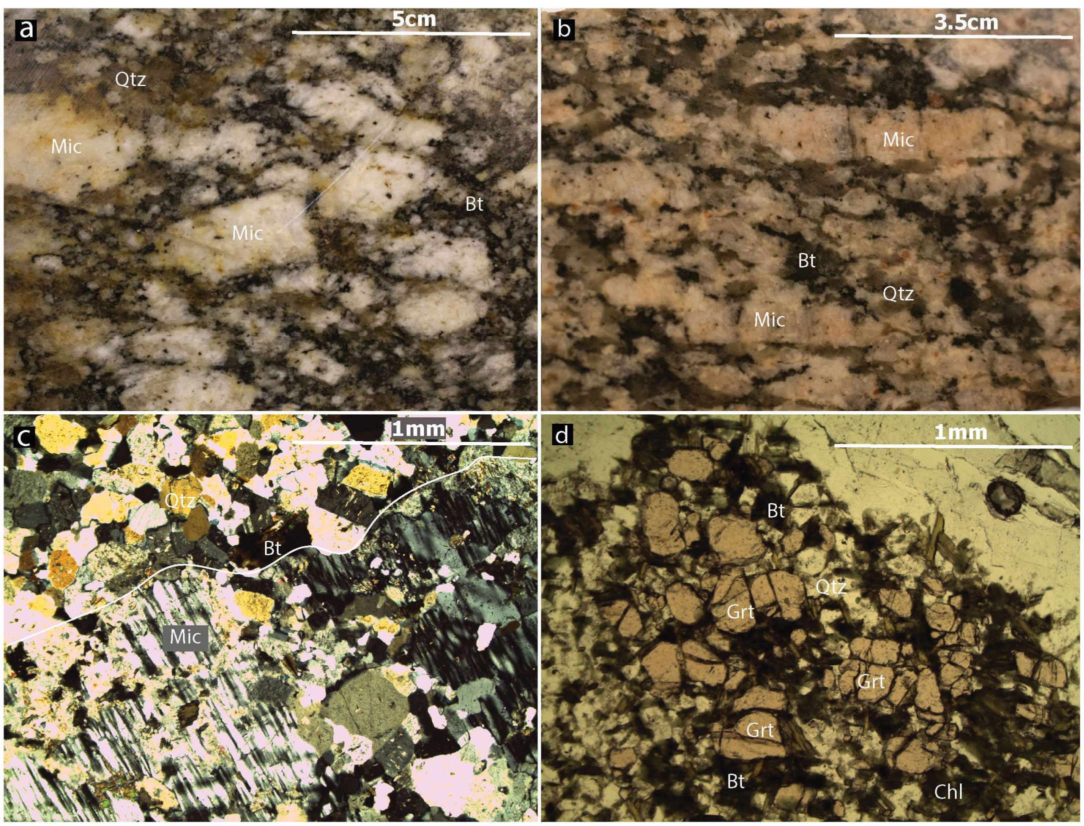


**Figure 2** Photographs of the Bell Creek Assemblage. **a** Hand sample photo of BCG-1A, white microcline (*Mic*) megacrysts in a fabric. **b** Hand sample photo of CLG-14B, pink microcline megacrysts in a fabric. **c** Photomicrograph of CCG-6A, microcline megacrysts (outlined in white) with inclusions of quartz (*Qtz*) and biotite (*Bt*) and secondary recrystallized quartz. **d** Photomicrograph of a mafic clot from BCG-8A biotite, chlorite (*Chl*), quartz and garnet (*Grt*), plane polarized light.

(24-40%), microcline (35-50%), plagioclase (10-20%), and biotite (3-10%). The main accessory (<1%) minerals are zircon, apatite, and magnetite. The microcline megacrysts are subhedral and host a variety of inclusions such as quartz, plagioclase, microcline, biotite, and zircon (Figure 2c). About 75% of microcline megacrysts exhibit perthitic exsolution while other megacrysts have Carlsbad twins or tartan twinning. Muscovite and chlorite are secondary mineral phases formed during post-emplacement alteration events. Post-emplacement alteration in some samples is notable where the igneous-formed biotite has altered to chlorite, and igneous-formed plagioclase phenocrysts have been partially altered to muscovite. There is secondary recrystallized quartz present in all samples as veins <0.25mm (Figure 2c). The samples BCG-8A, CCG-10A and CCG-1A have disseminated mafic clots composed of biotite, chlorite, garnet and quartz which are randomly oriented and range in size from 1-3mm (Figure 2d).

## 4.2 Bulk Rock Geochemistry

The major and trace element bulk rock geochemistry for each sample is given in Table 1. The granitoids have been separated into five subgroups based on Hoffman's (1987) classifications (Figure 3). Despite the granitoids being in subgroups, based on variations in hand-specimen textures and mineralogies, they plot similarly based on geochemistry. The Bell Creek granitoids plot as slightly peraluminous volcanic arc/syn-collisional granites based on their Al/(Na+K) vs Al/(Ca+Na+K) and Nb vs. Y, respectively (Figure 3b, 3c). They are I-type granites based on their Zr (ppm) and $10^4$Ga/Al (Figure 3d).

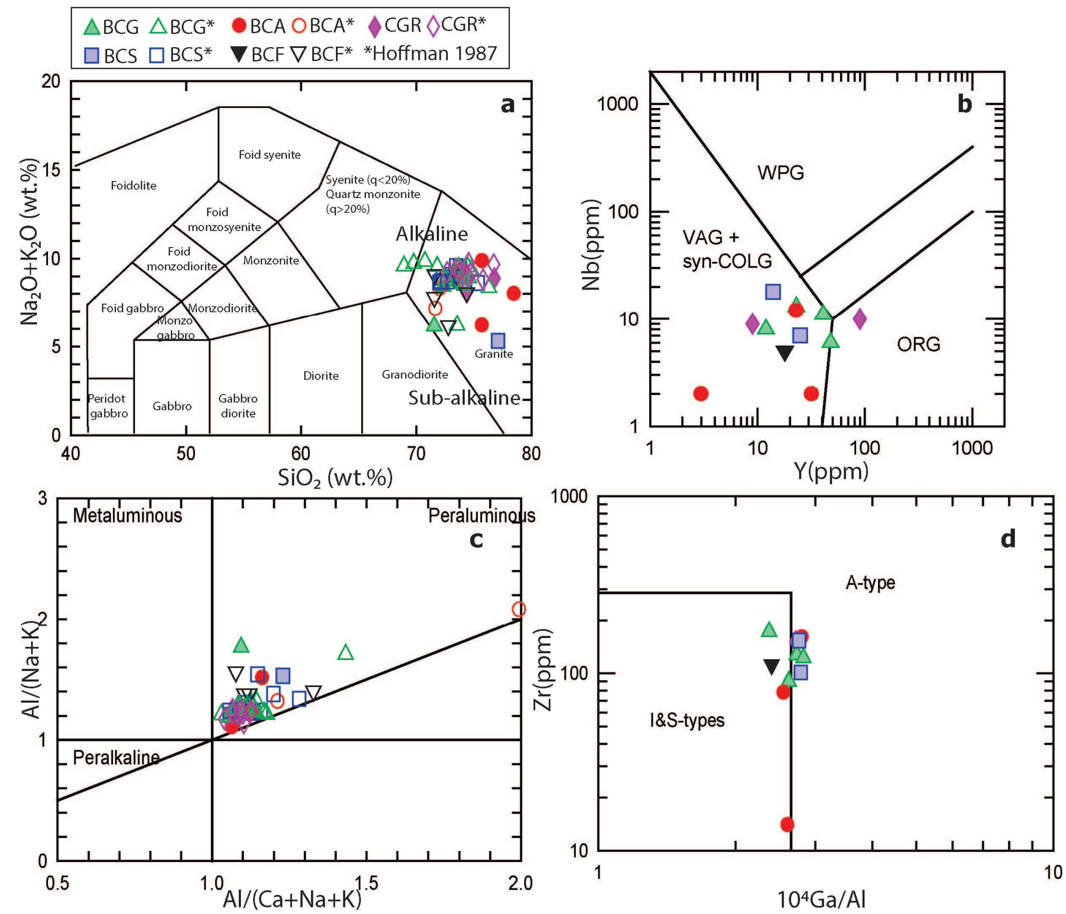


**Figure 3** Geochemical classification of bulk rock for the Bell Creek Assemblage (includes data from Hoffman, 1987). Bell Creek Granitoid (BCG); Foliated Bell Creek Granitoid (BCS); Altered Bell Creek Granitoid (BCA); Fine-grained Bell Creek Granitoid (BCF); Clotted Granitoids (CGR). **a** Total alkali ($Na_2O+K_2O$) versus silica diagram *modeled after Middlemost*, 1994. **b** Nb versus Y diagram (WPG: within plate granites, ORG: ocean ridge granites, VAG: volcanic arc granites, syn-COLG: syn-collisional granites); *after Pearce et al. 1984*. **c** Shand's index [$Al_2O_3/(Na_2O+K_2O)$] versus [$Al_2O_3/(CaO+Na_2O+K_2O)$] *classification diagram after Maniar and Piccolo 1989.* **d** Zr versus $10^4$Ga/Al *diagram after Whalen et al 1987.*

**Table 1** Major element chemistry and trace elements (ppm) for the Bell Creek Assemblage.

| Sample | BCG-1A | BCG-7A | CCG-1B | CCG-1A | BCG-8A | CCG-12A | CCG-9D | CLG-14B | BCG-4A | CCG-6A | BCG-8B | CCG-10A | CCG-9E | BCG-7C |
|---|---|---|---|---|---|---|---|---|---|---|---|---|---|---|
| Subgroup | BCG | BCA | BCG | CGR | CGR | BCG | BCS | BCG | BCG | BCF | BCA | CGR | BCA | BCS |
| $SiO_2$ | 70.5 | 74.7 | 62.6 | 75.7 | 73.3 | 71.3 | 71.3 | 71.8 | 73.0 | 72.5 | 77.4 | 72.9 | 74.7 | 76.1 |
| $Al_2O_3$ | 15.9 | 13.5 | 22.1 | 12.6 | 13.2 | 13.8 | 14.3 | 13.7 | 13.4 | 13.4 | 12.3 | 13.8 | 12.6 | 11.0 |
| $Fe_2O_3$ | 1.74 | 2.20 | 1.10 | 1.37 | 3.08 | 2.25 | 1.75 | 1.98 | 1.85 | 1.85 | 1.16 | 1.78 | 1.72 | 3.15 |
| MnO | 0.03 | 0.03 | 0.02 | 0.07 | 0.08 | 0.02 | 0.02 | 0.06 | 0.02 | 0.03 | 0.02 | 0.02 | 0.05 | 0.05 |
| MgO | 0.39 | 0.84 | 0.32 | 0.23 | 0.51 | 0.44 | 0.52 | 0.33 | 0.41 | 0.60 | 0.27 | 0.23 | 0.25 | 2.70 |
| CaO | 3.04 | 1.48 | 4.38 | 0.54 | 1.01 | 0.94 | 0.77 | 0.88 | 0.89 | 0.57 | 0.53 | 0.92 | 0.26 | 0.96 |
| $Na_2O$ | 4.53 | 4.22 | 6.59 | 2.20 | 3.53 | 2.94 | 3.67 | 3.27 | 2.79 | 3.09 | 2.54 | 3.40 | 1.54 | 2.84 |
| $K_2O$ | 1.45 | 1.81 | 1.70 | 6.50 | 4.39 | 5.30 | 5.07 | 5.25 | 5.62 | 5.81 | 5.00 | 5.27 | 8.14 | 2.30 |
| $TiO_2$ | 0.23 | 0.24 | 0.09 | 0.01 | 0.21 | 0.21 | 0.20 | 0.14 | 0.22 | 0.16 | 0.07 | 0.16 | 0.09 | 0.21 |
| $P_2O_5$ | 0.04 | 0.01 | 0.02 | 0.04 | 0.03 | 0.05 | 0.03 | 0.02 | 0.05 | 0.04 | 0.04 | 0.01 | 0.04 | 0.08 |
| LOI | 0.8 | 1.0 | 1.1 | 0.7 | 1.0 | 1.0 | 0.6 | 0.7 | 1.0 | 1.0 | 0.7 | 0.5 | 0.6 | 0.7 |
| Total | 98.7 | 100.0 | 100.0 | 100.0 | 100.3 | 98.3 | 98.1 | 98.1 | 99.2 | 99.0 | 100.0 | 99.0 | 100.0 | 99.9 |
| Trace Elements (ppm) | | | | | | | | | | | | | | |
| Sc | 3 | 3 | 1 | 5 | 8 | 4 | 3 | 5 | 2 | 3 | 1 | 3 | 4 | 2 |
| Be | 7 | 2 | 3 | 2 | < 1 | 2 | 1 | 1 | 1 | 1 | 1 | < 1 | < 1 | < 1 |
| V | 16 | < 5 | 11 | < 5 | < 5 | 11 | 8 | 6 | 11 | 7 | < 5 | < 5 | < 5 | 14 |
| Ba | 169 | 447 | 351 | 1001 | 673 | 699 | 782 | 453 | 990 | 829 | 412 | 223 | 727 | 284 |
| Sr | 170 | 172 | 482 | 92 | 76 | 73 | 93 | 54 | 100 | 71 | 82 | 42 | 98 | 51 |
| Y | 23 | 23 | 3 | 26 | 90 | 41 | 25 | 48 | 12 | 18 | 3 | 9 | 32 | 14 |
| Zr | 172 | 160 | 133 | 6 | 151 | 127 | 101 | 90 | 122 | 112 | 14 | 7 | 78 | 153 |
| Cr | < 20 | 80 | < 20 | 70 | < 20 | 80 | 60 | < 20 | < 20 | 70 | < 20 | 60 | < 20 | < 20 |
| Co | 3 | 3 | 2 | 1 | 2 | 2 | 2 | 1 | 2 | 3 | < 1 | 1 | 1 | 4 |
| Ni | < 20 | < 20 | < 20 | < 20 | < 20 | < 20 | < 20 | < 20 | < 20 | < 20 | < 20 | < 20 | < 20 | < 20 |
| Cu | < 10 | < 10 | < 10 | < 10 | < 10 | < 10 | < 10 | < 10 | < 10 | < 10 | < 10 | < 10 | < 10 | < 10 |
| Zn | 30 | < 30 | < 30 | < 30 | 30 | 50 | < 30 | 40 | 30 | < 30 | < 30 | 30 | < 30 | 50 |
| Ga | 20 | 20 | 26 | 15 | 19 | 20 | 21 | 19 | 20 | 17 | 17 | 21 | 17 | 16 |
| Ge | < 1 | 1 | < 1 | 2 | 2 | < 1 | < 1 | < 1 | < 1 | < 1 | 2 | < 1 | 2 | 1 |
| As | < 5 | 5 | < 5 | < 5 | < 5 | < 5 | < 5 | < 5 | < 5 | < 5 | < 5 | < 5 | < 5 | < 5 |
| Rb | 64 | 68 | 28 | 117 | 145 | 226 | 113 | 183 | 201 | 144 | 159 | 163 | 204 | 101 |
| Nb | 13 | 12 | 2 | < 1 | 10 | 11 | 7 | 6 | 8 | 5 | 2 | 9 | 2 | 18 |
| Mo | < 2 | < 2 | < 2 | < 2 | < 2 | < 2 | < 2 | < 2 | < 2 | < 2 | < 2 | < 2 | < 2 | < 2 |
| Ag | 0.6 | 0.7 | < 0.5 | < 0.5 | < 0.5 | < 0.5 | < 0.5 | < 0.5 | < 0.5 | < 0.5 | < 0.5 | < 0.5 | < 0.5 | 0.6 |
| In | < 0.2 | < 0.2 | < 0.2 | < 0.2 | < 0.2 | < 0.2 | < 0.2 | < 0.2 | < 0.2 | < 0.2 | < 0.2 | < 0.2 | < 0.2 | < 0.2 |

Table 1 (*Continued*)

| Sample | BCG-1A | BCG-7A | CCG-1B | CCG-1A | BCG-8A | CCG-12A | CCG-9D | CLG-14B | BCG-4A | CCG-6A | BCG-8B | CCG-10A | CCG-9E | BCG-7C |
|---|---|---|---|---|---|---|---|---|---|---|---|---|---|---|
| Sn | 2 | 1 | < 1 | < 1 | < 1 | 2 | < 1 | 2 | 3 | 10 | < 1 | 1 | < 1 | 3 |
| Sb | < 0.5 | 3.2 | < 0.5 | 1.8 | 0.9 | < 0.5 | < 0.5 | < 0.5 | < 0.5 | < 0.5 | < 0.5 | < 0.5 | < 0.5 | < 0.5 |
| Cs | 0.7 | < 0.5 | 0.6 | < 0.5 | < 0.5 | 0.7 | < 0.5 | < 0.5 | < 0.5 | < 0.5 | < 0.5 | < 0.5 | < 0.5 | < 0.5 |
| La | 68.3 | 79.9 | 51.9 | 7.2 | 86.1 | 80.4 | 76 | 61.3 | 75.6 | 65 | 8.8 | 7.1 | 37.1 | 65.7 |
| Ce | 121 | 142 | 83.7 | 10.7 | 156 | 147 | 137 | 115 | 132 | 112 | 13.7 | 9.6 | 67.3 | 118 |
| Pr | 11.8 | 13.6 | 7.69 | 1.04 | 15.2 | 14.4 | 13.4 | 11.5 | 12.7 | 11 | 1.22 | 0.8 | 6.53 | 12 |
| Nd | 40.3 | 44.8 | 24.9 | 3.2 | 51.5 | 48.9 | 44.8 | 40.1 | 42.9 | 37.6 | 3.8 | 2.2 | 23.1 | 37.5 |
| Sm | 7.9 | 8 | 4.3 | 0.7 | 9.9 | 9.6 | 8.6 | 7.8 | 7.7 | 7.1 | 0.7 | 0.5 | 4.2 | 6.9 |
| Eu | 0.99 | 0.59 | 1.73 | 0.47 | 0.74 | 0.67 | 0.7 | 0.46 | 0.73 | 0.82 | 0.48 | 0.25 | 0.48 | 0.66 |
| Gd | 6.1 | 6.4 | 2.4 | 0.8 | 8.7 | 7.4 | 6.3 | 6.1 | 5.1 | 5 | 0.5 | 0.6 | 3.5 | 5.2 |
| Tb | 0.9 | 0.9 | 0.3 | 0.2 | 1.6 | 1.2 | 1 | 1 | 0.7 | 0.7 | < 0.1 | 0.2 | 0.6 | 0.7 |
| Dy | 5 | 5.2 | 1 | 2.8 | 11.8 | 7.5 | 5.1 | 6.9 | 3.2 | 3.8 | 0.6 | 1.2 | 4.3 | 3.6 |
| Ho | 0.9 | 0.9 | 0.1 | 1 | 3 | 1.4 | 0.8 | 1.6 | 0.4 | 0.7 | 0.1 | 0.3 | 1.1 | 0.6 |
| Er | 2.4 | 2.1 | 0.3 | 4.6 | 11.3 | 3.5 | 1.8 | 5.6 | 1 | 1.8 | 0.3 | 0.8 | 4.2 | 1.3 |
| Tm | 0.32 | 0.28 | < 0.05 | 0.91 | 1.87 | 0.42 | 0.2 | 0.98 | 0.12 | 0.24 | < 0.05 | 0.13 | 0.8 | 0.15 |
| Yb | 2 | 1.5 | 0.3 | 7.3 | 12.2 | 2.3 | 1.1 | 7.2 | 0.7 | 1.5 | 0.2 | 0.8 | 5.4 | 0.9 |
| Lu | 0.31 | 0.2 | < 0.01 | 1.34 | 1.75 | 0.32 | 0.14 | 1.13 | 0.1 | 0.22 | < 0.01 | 0.11 | 0.91 | 0.14 |
| Hf | 4.9 | 5.1 | 3.8 | 0.4 | 4.8 | 3.8 | 2.8 | 3 | 3.7 | 3.2 | 0.7 | 0.3 | 2.6 | 4.4 |
| Ta | 4.4 | 1.3 | 0.1 | < 0.1 | 0.7 | 0.9 | 0.7 | 1 | 1.1 | 0.3 | 0.2 | 1 | 0.3 | 1.3 |
| W | 2 | < 1 | 5 | < 1 | < 1 | < 1 | < 1 | < 1 | < 1 | 2 | < 1 | < 1 | < 1 | < 1 |
| Tl | 0.3 | < 0.1 | < 0.1 | < 0.1 | 0.1 | 1.1 | 0.4 | 0.9 | 0.9 | 0.6 | 0.2 | 0.6 | 0.3 | 0.5 |
| Pb | 76 | 52 | 39 | 48 | 77 | 88 | 41 | 75 | 56 | 69 | 48 | 51 | 200 | 32 |
| Bi | < 0.4 | < 0.4 | < 0.4 | < 0.4 | < 0.4 | < 0.4 | < 0.4 | < 0.4 | < 0.4 | < 0.4 | < 0.4 | < 0.4 | < 0.4 | < 0.4 |
| Th | 56.2 | 58.5 | 22.3 | 2 | 66.7 | 60.8 | 56.7 | 47 | 52.6 | 52.4 | 4.6 | 5.6 | 30.6 | 49.5 |
| U | 30.8 | 10.7 | 2.2 | 1.5 | 21.1 | 9.7 | 8.3 | 17.4 | 7 | 32.9 | 6.6 | 2.8 | 15.8 | 7.3 |

BCG: Normal Bell Creek Granite; BCS: Foliated Bell Creek Granite; BCA: Altered Bell Creek Granite; BCF: Fine-grained Bell Creek Granite; CGR: Clotted Bell Creek Granite.

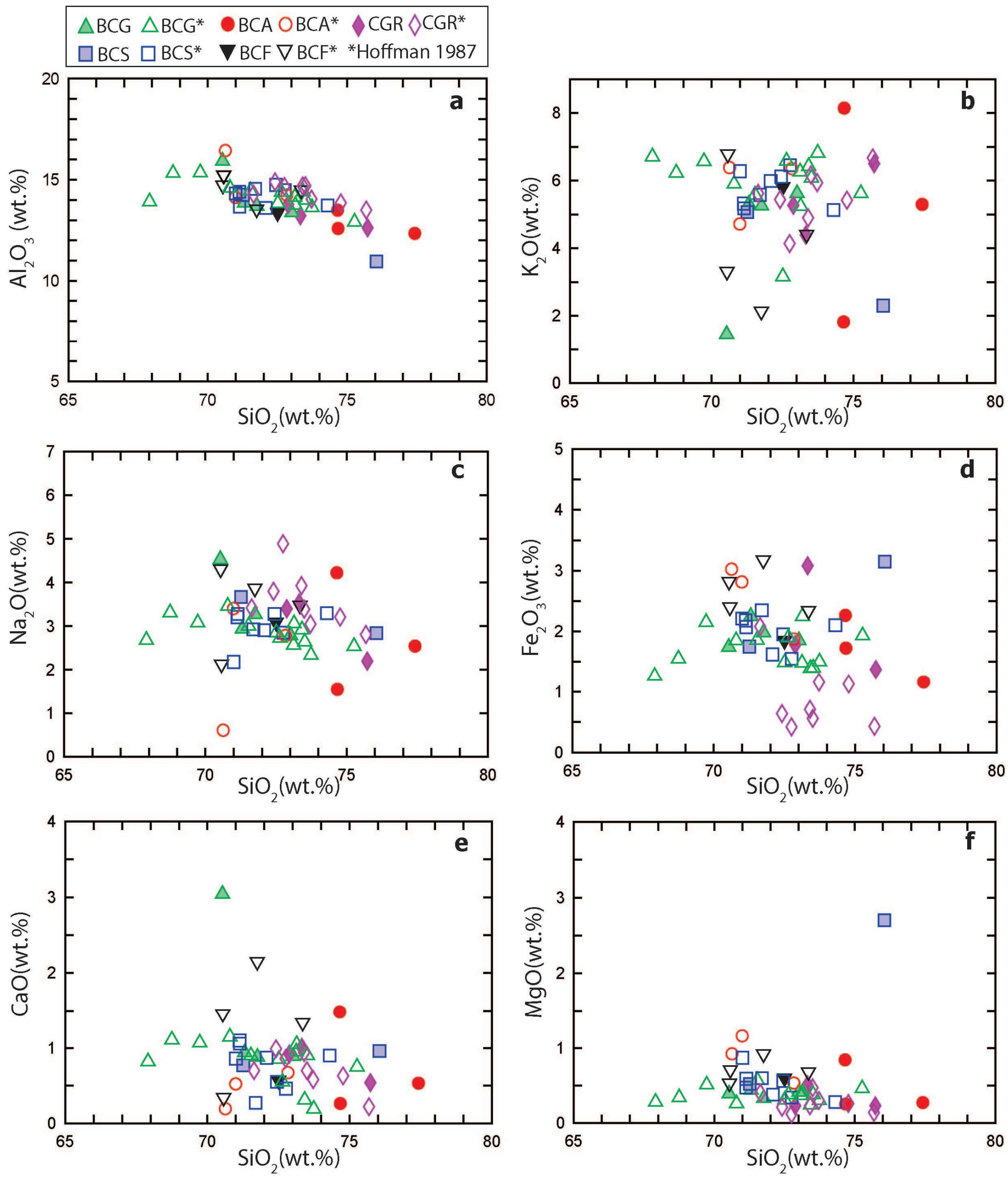


**Figure 4** Covariation diagrams of selected bulk rock major oxides versus silica; includes data from Hoffman (1987). Bell Creek Granitoid (BCG); Foliated Bell Creek Granitoid (BCS); Altered Bell Creek Granitoid (BCA); Fine-grained Bell Creek Granitoid (BCF); Clotted Granitoids (CGR).

## 4.3 Trace Element Geochemistry

In general, the granitoids are enriched in LREEs relative to MREEs and HREEs (Figure 5). Most of the granitoids have a -Eu anomaly but the following group of samples; CCG-1A, CCG-10A and BCG-8B, have a +Eu anomaly; these samples range in $SiO_2$ from 74-77% (Figure 5). The +Eu samples are lower in LREEs and HREEs as compared to -Eu anomaly samples(Figure 5). The +Eu samples have lower Zr concentrations that range from 6-14ppm, as compared to the rest of the granitoids which have a range of zircon from 78-172ppm (Table 1).

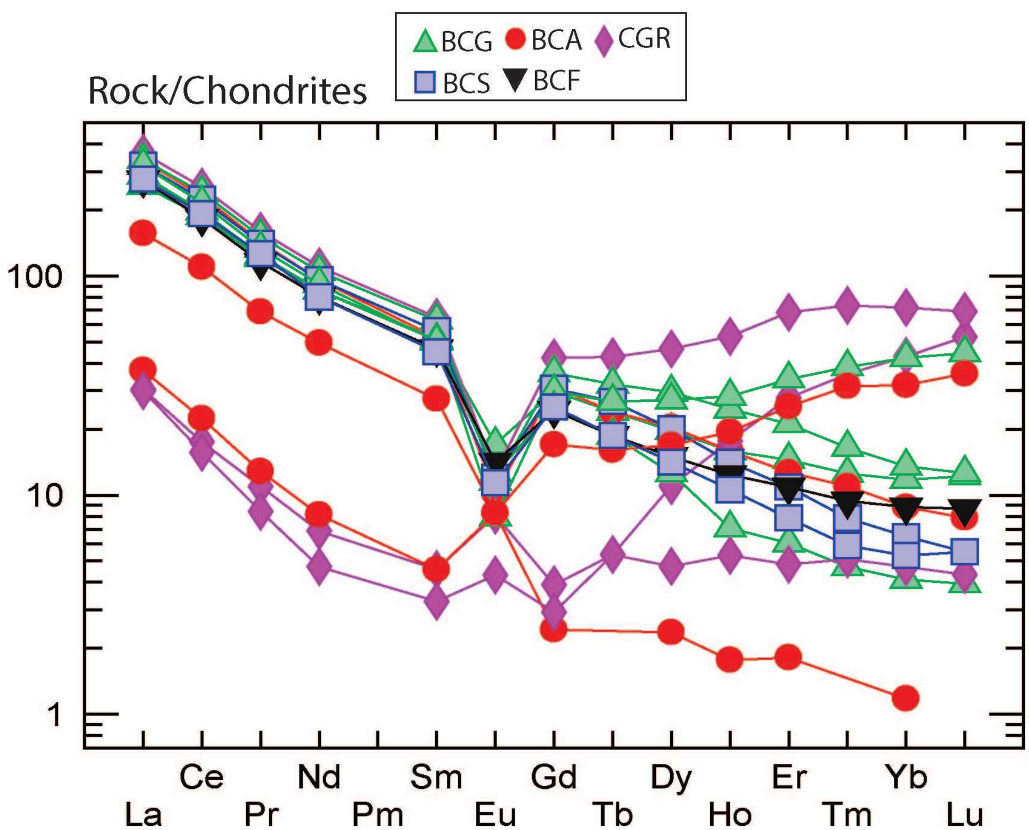


**Figure 5** Chondrite-normalized REE patterns for the Bell Creek granitoids. *Chondrite normalizing values are from Sun and McDonough 1989*.

The Bell Creek granitoids subgroups have similar trace element, there are no major distinctions between the subgroups, aside from a couple outliers (Figure 6). The granitoids display a Sr/Y ratio less than 10 except for one +Eu sample with a slightly higher ratio of ~27 (Figure 6). In general, the granitoids are enriched in the LILE (represented by Ba) and have Rb/Sr ratios ranging from 0.5 to 7 (Figure 6).

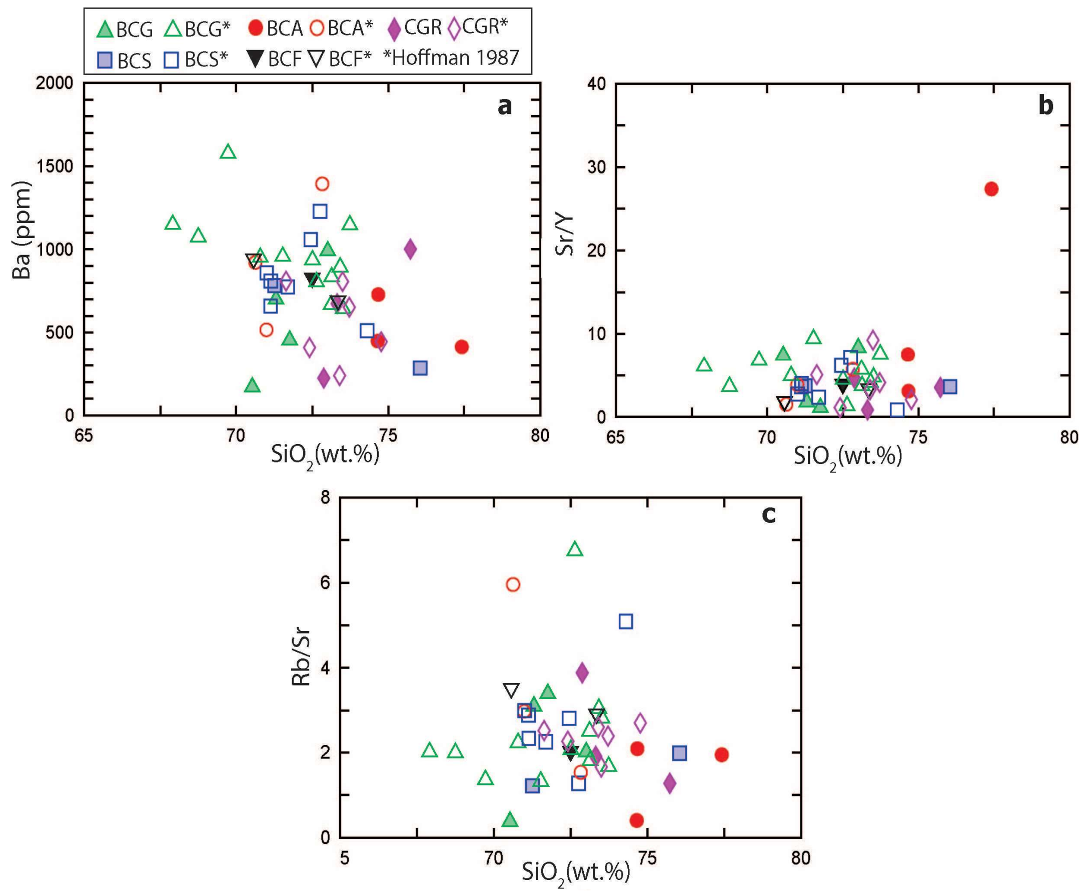


**Figure 6** Covariation diagrams of selected whole rock trace elements versus silica; includes mafic samples and data from Hoffman (1987). Bell Creek Granitoid (BCG); Foliated Bell Creek Granitoid (BCS); Altered Bell Creek Granitoid (BCA); Fine-grained Bell Creek Granitoid (BCF); Clotted Granitoids (CGR).

## 4.4 Zircon Analyses

Thirteen of representative granitoids were chosen for in-situ zircon U-Pb dating, Lu-Hf isotopic analysis, and oxygen isotopic analysis. The representative granitoids included a selection from each subgroup studied, normal Bell Creek granite, foliated Bell Creek granite, altered Bell Creek granite, fine-grained Bell Creek granite and clotted Bell Creek granite. The analytical results for the U-Pb and the calculated ages are provided in Appendices 5-8.

Zircon grains are mostly colorless, with some having an orange/red tint. Zircon grains have been sorted into igneous, metamorphic and inherited groups based on U-Pb ages and grain morphology (Figure 7). Grains have a variety of shapes and include a mix of those that are thin and elongate (50µm x 200µm) or short and stubby (75µm x 125µm). Most grains have well developed terminated ends (noticeably sharp crystal faces as seen in Figure 7.2c), but others have a rounded morphology (boundaries of grain are smooth as seen in Figure 7.1c). Zircon grain size varies for each rock sample, all zircon grains are between 60 and 200µm, but most are 100-130µm. Backscatter electron (BSE) images of representative zircons reveal a variety of internal structures (Figure 7). Many grains exhibit oscillatory zoning (Figure 7.1a) and xenocrystic or inherited cores (Figure 7.2a). All grains exhibit some secondary textures such as fractures, healed cracks (Figure 7.1d & 7.4b) and metamict zones (Figure 7.3a); these areas were avoided for analysis.

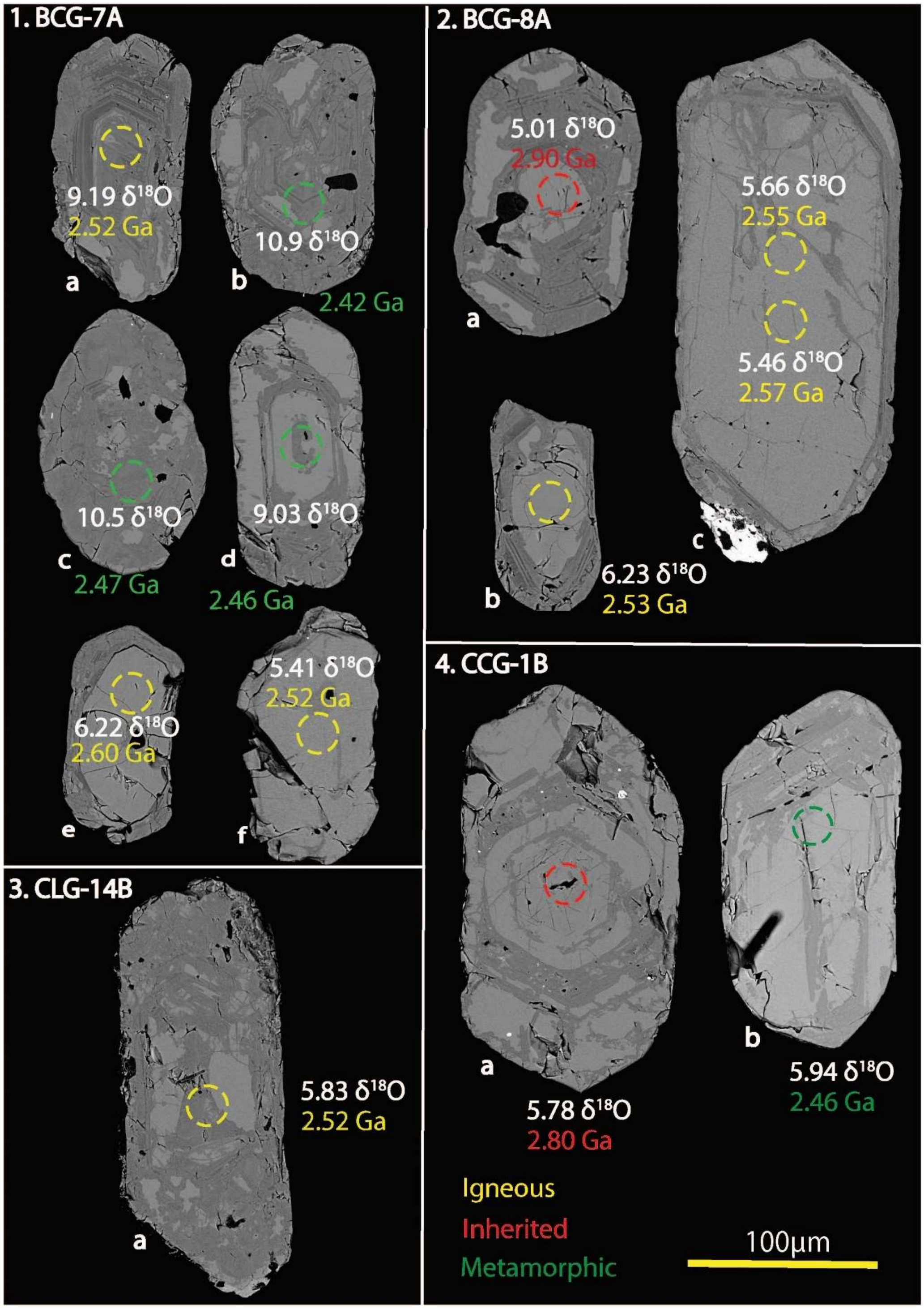


**Figure 7** Backscattered electron images of zircon from selected Bell Creek Granite samples. The circles represent the analysis location for oxygen and U-Pb data. **2a** and **4a** represent inherited zircons with xenocrystic cores.**1a**- concentric growth pattern. **1b**-Convolute zoning pattern. **1e** and **2b** concentric zone metamorphic overgrowth around core.

**Table 2** Summary of U-Pb crystallization age for each rock sample.

| Rock Type Subgroup | Sample Name | U-Pb Crystallization Age (Ga) | Inherited Grains (Ga) | Metamorphic Grains (Ga) |
|---|---|---|---|---|
| *Normal Bell Creek* | CLG-14B | 2.42 ± 0.042 | 3.1, 3.6, 2.8 | 2.3 |
| | CCG-12A | 2.43 ± 0.160 | 2.7 | 2.0 |
| | BCG-4A | 2.51 ± 0.021 | 2.8, 3.0, 3.1, 3.5, 3.9, 4.2 | |
| | BCG-1A | 2.58 ± 0.056 | 2.7, 2.8 | 2.3, 2.4 |
| *Foliated Bell Creek* | CCG-9D | 2.59 ± 0.028 | 3.3, 3.5 | |
| *Altered Bell Creek* | BCG-7C | 2.61 ± 0.047 | 2.7, 2.8, 2.9, 3.1, 3.3 | 2.3, 2.4, |
| | CCG-9E | 2.56 ± 0.038 | 2.7, 2.8 | 2.3, 2.4 |
| | BCG-8B | 2.54 ± 0.040 | 3.1 | |
| *Fine-grained Bell Creek* | CCG-6A | 2.53 ± 0.070 | | 2.3, 2.4 |
| *Clotted Bell Creek* | BCG-8A | 2.55 ± 0.017 | 2.7, 2.9 | 2.2, 2.3 |
| | CCG-1A | 2.55 ± 0.033 | 2.7, 3.2 | 1.8, 2.3 |

*Crystallization mean age is determined by calculating the weighted mean for each sample for concordant igneous grains, example can be seen in Figure 8

The best estimate of the magmatic crystallization age is the U-Pb calculated mean age which is between 2.5 and 2.6 Ga for the Bell Creek granitoids, individual mean ages (calculated with isoplot) are shown in Table 2 and a representative concordia plot in Figure 8. Many samples have a range of discordant ages representing inherited and metamorphic grains (Table 2). Inherited grains were identified by core analyses that had a distinct difference in U-content between the core and the rim resulting in an older U-Pb date for the core. Xenocrystic cores have a rounded morphology and tend to have zoned magmatic overgrowths (Figure 7.2a, 7.4a). Sample BCG-4A, normal Bell Creek sample, has the widest variety of inherited grains ranging from 2.8-4.2 Ga. Metamorphic grains, zircons which grew during metamorphic events after the crystallization of the Bell Creek granitoids, were identified by having young U-Pb ages compared to the mean age for the Bell Creek granitoids (Figure 7). Metamorphic zircon ages for the suite reflect metamorphic events at the following time periods 1.8- 2.0 Ga, and 2.2-2.3 Ga (Table 2).

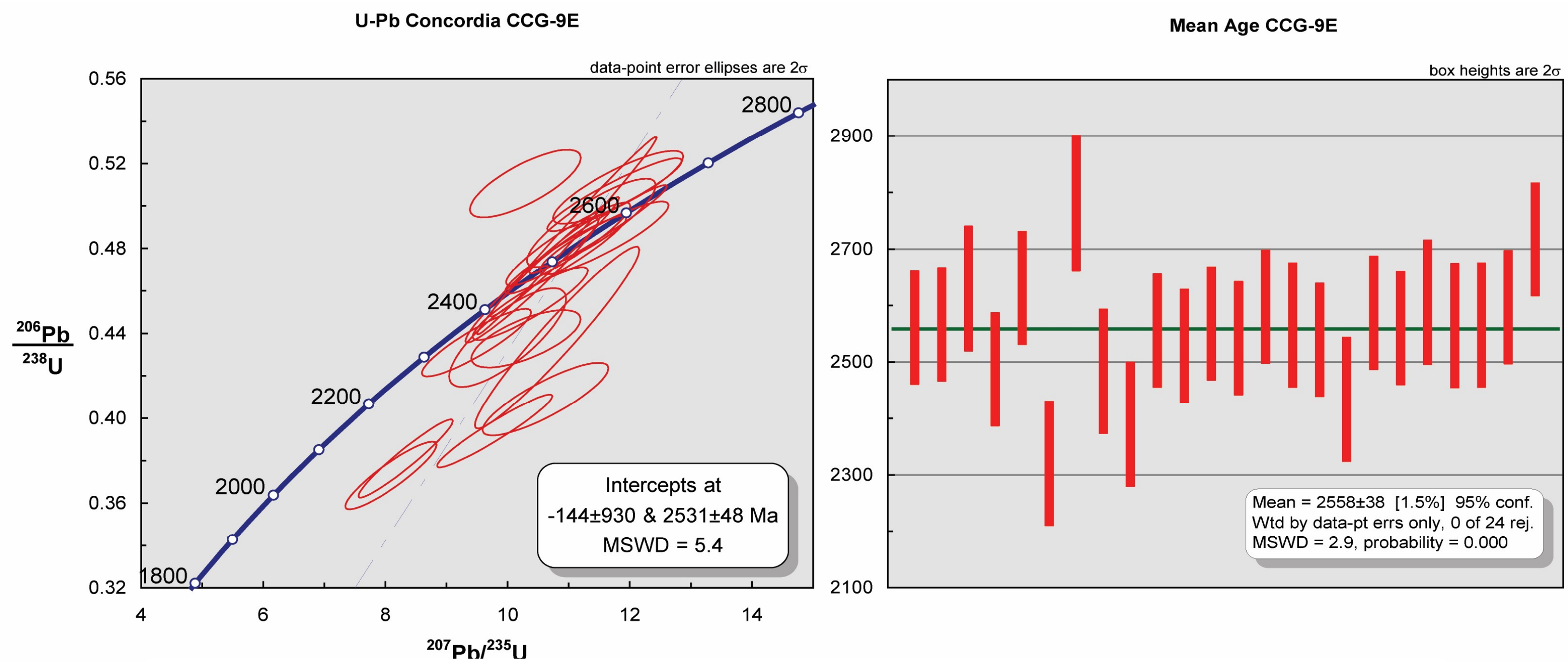


**Figure 8** Zircon U-Pb concordia diagram and weighted mean age of CCG-9E.

Variations in εHf(t) and $\delta^{18}O$ (VSMOW) are shown in Figure 9 and organized by the zircon grain classification as igneous, inherited or metamorphic on the bases of ages and grain morphology; data are provided in Appendices 5 and 7. The mean εHf(t) value for the Bell Creek assemblage is -12.4. The range is from -30 to +30 εHf(t) with the majority between -15 and -5 εHf(t) (Figure 9). The difference in classification of zircon grain type (igneous, inherited, or metamorphic) does not have an effect on εHf(t)

The $\delta^{18}O$ values range from +4.0‰ to +13.0‰, with a mean value of 6.08‰ (Figure 9). The igneous and inherited grains tend to have lower $\delta^{18}O$ values than the metamorphic grains (Figure 9). The majority of $\delta^{18}O$ values for the igneous zircons are less than +6‰ (Figure 9). The average $\delta^{18}O$ value for the inherited zircons is +5‰, as compared to the $\delta^{18}O$ of the metamorphic zircons which are greater than +6‰ (Figure 9).

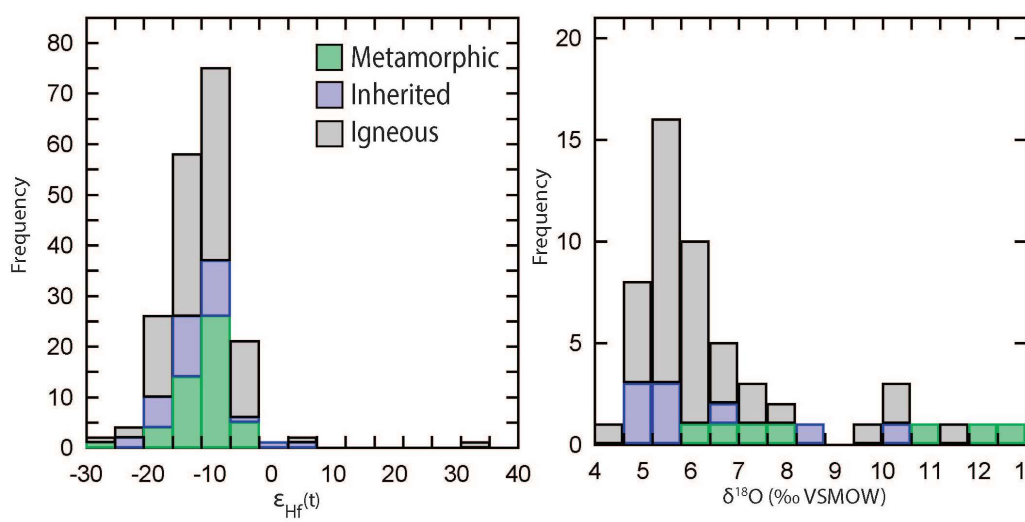


**Figure 9** Histograms showing the frequency of εHf(t) and $\delta^{18}O$ (‰ VSMOW) for Bell Creek Granitoids.

# 5 Discussion

## 5.1 Bell Creek Granite U-Pb Zircon Ages

There have been several previous studies that have attempted to obtain the crystallization age of the Bell Creek assemblage. The first attempt was by Van Schmus & Woolsey (1975) based on whole-rock Rb/Sr isotopes and yielded an age range between 2.8-2.5 Ga; although this method has been shown not to be reliable for Precambrian rocks (Waight, 2015). Tinkham (1997) estimated the age of the Bell Creek assemblage to be ~2.6 Ga, based on three discordant U-Pb zircon ages.

In this study, we have compiled a comprehensive examination of a suite of different rocks that are representative of the spectrum variability in the Bell Creek assemblage including: Normal Bell Creek Granite, Foliated Bell Creek Granite, Altered Bell Creek Granite, Equigranular Bell Creek Granite and Fine-grained Bell Creek Granite. These granites vary in bulk-rock major and trace element geochemistry (Figure 3; Table 1; Figure 4). The data presented here (Table 2) indicates the age for the Bell Creek assemblage is between 2.5 and 2.6 Ga based on multiple U-Pb zircon ages. This is consistent within the age determined by Tinkham (1997).

The large population of zircon ages obtained for this study include, in addition to magmatic zircon grains a number of inherited zircon grains with ages older than the emplacement age and a lesser number of zircon grains with ages younger than the emplacement age corresponding to regional Paleoproterozoic metamorphic events. The majority of inherited zircon grains are only slightly older than the crystallization age at 2.7

Ga. Other inherited grains can be grouped into time intervals of 2.8 Ga, 3.0-3.1 Ga, 3.5-3.6 Ga, 3.9 Ga and 4.2 Ga (Table 2). The ages of younger metamorphic related zircon grains can be grouped into time intervals of 1.8 Ga and 2.2-2.3 Ga.

### 5.1.1 Inherited Zircon Origin

While there were many inherited zircon ages, the most prominent zircon age group was at 2.7 Ga. These zircon grains are possibly related to the collision of the Southern Complex with the GLTZ proposed by Sims (1991). The 2.8 Ga zircon grains could be remnants from the Twin Lake Assemblage which lies east of the Bell Creek Assemblage and has an age of 2.8 (Tinkham, 1997). Additionally, Tinkham (1997) dated a 3.1 Ga zircon in the Twin Lake Assemblage suggesting there were more rocks in the Southern Complex which were at least 3.1 Ga. The nearby Minnesota Archean Gneiss terrane is ~3.8 Ga (Ayuso et al, 2018), therefore, inherited zircons from this time range could be attributed to this neighboring terrane. A single concordant 4.2 Ga age zircon was obtained, but there is currently no evidence of rocks of this age cropping out in the United States.

### 5.1.2 Metamorphic Zircon Grain Origin

The metamorphic zircon grains found are possibly related to major metamorphic events that occurred in this area. The 1.8 Ga grains likely represent zircon growth during metamorphism related to the Penokean orogeny which occurred 1.87-1.83 Ga (Schulz & Cannon, 2007). The 2.2-2.3 Ga metamorphic zircon ages that were obtained could possibly represent zircon growth during metamorphism related to the deposition of the Marquette Range Supergroup volcanism (Vallini, 2006).

## 5.2 Petrogenesis

### 5.2.1 Continental Arc Magmatism

The Bell Creek granitoids plot as slightly peraluminous alkaline granites, are enriched in LREEs and have high concentrations of K, Rb, Ba and Th (Figure 3; Table 1) which are characteristics of continental arc magmas (Pearce and Parkinson, 1993). The Bell Creek granitoids plot as a syn-collisional volcanic arc granite based on classifications by Pearce et al. (1984; Figure 3).

Hoffman (1987) suggested that the Bell Creek assemblage is an S-type due to characteristic chemical (ACF diagrams, Zr vs $SiO_2$, CaO vs $SiO_2$, Ba vs $SiO_2$ and Sr vs $SiO_2$; based on Hine, et al., 1978) and mineralogical features (presence of garnet, monazite, ilmenite) that reflect the process of partial melting of a sedimentary protolith. However, the Bell Creek granitoids are actually only slightly peraluminous, whereas S-type granites are strongly peraluminous and typically contain abundant cordierite, muscovite, garnet and sillimanite which is absent in the Bell Creek granitoids as primary magmatic phases. The S-type characteristics Hoffman (1987) observed are instead interpreted to be a signature of assimilated pelitic crustal material, not primary signatures from the source material.

### 5.2.2 Source Characteristics

Hoffman (1987) proposed the source rock for the Bell Creek assemblage was an amphibolite which was likely to have formed by metamorphism of a mafic igneous rock at depth. Beard & Lofgren (1991) demonstrated that partial melting of an amphibolite can produce granitic melt that is slightly peraluminous at middle- to lower-crustal conditions, similar to the Bell Creek Granitoids. The Bell Creek granitoids show the characteristic middle rare-earth element depletion that would develop if amphibole were in the source (Figure 10). Experiments by Moyen (2009) show that amphibole was not a stable restite phase in dehydration melting except under the highest-pressure conditions. However, in water-saturated experiments, amphibole was present as a restite phase. The relatively low Sr/Y ratio (Figure 6b) implies there was also little to no garnet in the source rock. The pressure conditions for partial melting to produce Bell Creek Granite could have occurred under lower crustal conditions (<35km) with amphibole as a restite phase (Zhang et al., 2013). Zhang et al. (2013) showed that melting of an amphibolite at 7kb under water-saturated or under-saturated conditions would be in equilibrium with up to 40% melt. The high viscosity of silica-rich magmas; however, would greatly hinder the movement of this magma through the crust from where it was formed to where it was emplaced. Therefore, it is likely that an intermediate magma (e.g. tonalitic or dioritic) was actually produced, which eventually fractionated further in the shallower crust to ultimately form the granite. There is evidence of intermediate compositions in the area; tonalite and diorite have been mapped in the Southern Complex (Gair and Thaden 1968) and nearby in the Northern Complex (Wilkin & Bornhorst 1992).

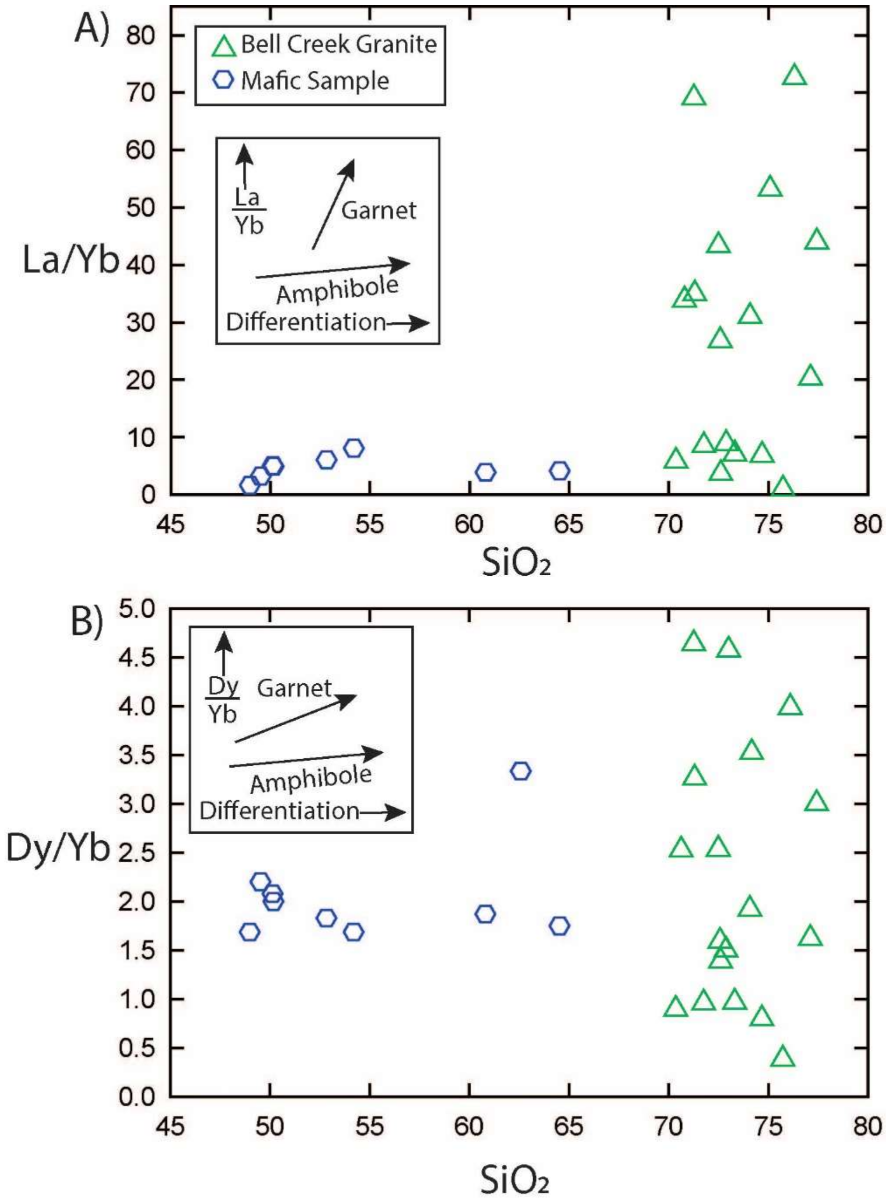


**Figure 10** A: La/Yb vs. $SiO_2$. B: Dy/Yb vs. $SiO_2$. Data shown for Bell Creek Granite and local mafic samples defining differentiation trends. Arrows show expected fractionation effects for garnet and amphibole. Modified from Davidson et al. 2007.

### 5.2.3 Hf Isotopes

In recent years, Hf model ages of zircons have been used to estimate the age that the primary magma was initially extracted from the mantle (Amelin et al., 1999; Vervoort, 1999;2014, Chu et al., 2006; Belousova et al., 2010). Zircons preserve their initial $^{176}Hf/^{177}Hf$ ratio from the source magma at the time of crystallization (Hawkesworth and Kemp, 2006). This model age method uses the Lu/Hf ratio of the zircon to determine an average time since the zircon was crystallized, however, the Lu/Hf, of the source magma has to be estimated, usually the depleted mantle is used (Hawkesworth and Kemp, 2006; Vervoort, 2014).

The Hf model age for the Bell Creek granitoids is approximately 3.3 Ga (Figure 11). This model age would, therefore, represent the emplacement age of the presumed amphibolite protolith.

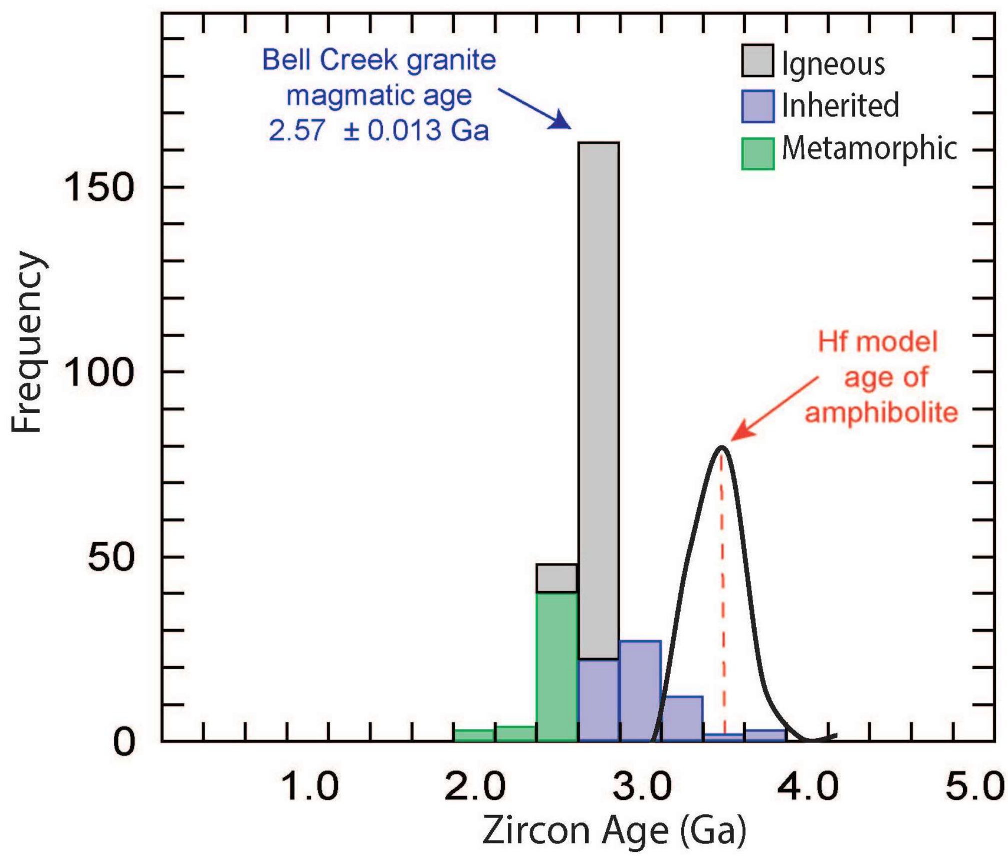


**Figure 11** Histogram of the U-Pb zircon ages sorted by grain type with the Hf model age overlaid.

## 5.3 Assimilation

The resulting granitoid produced by partial melting of an amphibolite would be low-K, therefore, in order to produce high-K calc-alkaline granitoids was likely a crustal contribution of pelitic material, rich in Al, Si and K (Roberts & Clemens, 1993). The K-rich nature of the Bell Creek Granitoids, therefore, must be related to assimilation of a pelitic source. The source of the assimilated pelitic material could have been graywacke, shale and/or arkose which is reasonable because Hoffman (1987) hypothesized that the Bell Creek granite was emplaced into a suite of deformed metasediments and metavolcanics.

A select number of the Bell Creek granitoids contain macroscopic clots of partially assimilated pelitic sedimentary material (Hoffman 1987; s*ee samples BCG-8A, CCG-10A & CCG-1A*). Hoffman (1987) also found thin layers of banded iron formation (BIF) as inclusions within the Bell Creek assemblage. If the Bell Creek granite was indeed emplaced into a suite of metasediments and metavolcanics the proposed assimilated pelitic material could have been associated with the BIF, both materials being deep ocean sediments. These clots are abundant and can be found throughout the Southern Complex in the Bell Creek assemblage. Hoffman (1987) described the clotted granites as a separate unit; however, they are geochemically the same as the Bell Creek granitoids (Figures 4 & 6). Therefore, the clotted granitoids appear to have preserved mascroscopic evidence of the assimilation of pelitic material, whereas the assimilated material has been completely digested in the most common Bell Creek granitoids.

The $\delta^{18}O$ values of zircon that are greater than 6.0‰ are particularly indicative of involvement of sedimentary rocks in the origin of the magma either as a source rock or as an assimilate (Valley, 2003). The Bell Creek $\delta^{18}O$ values in zircon reflect a range from mantle-like values ~5.5‰ to those between 6.0-13.0 ‰ (Figure 9). The Bell Creek O-Hf isotope data within an array that reflects mixing variations between different components: 1) -εHf and low (~5.5-6.0 ‰) $\delta^{18}O$ values that are consistent with mantle-derived magmas, and 2) -εHf and high (>6.0‰) $\delta^{18}O$ values that reflect a crustal source contribution (Figure 12). The wide range of $\delta^{18}O$ values in zircon from the primary igneous event at ~2.6 Ga can be interpreted as having captured different amounts of assimilation as the magma cooled. Some zircons grew early in the process, capturing lower mantle-like $\delta^{18}O$ values and as assimilation progressed zircons that grew later captured higher $\delta^{18}O$ values. This progression of $\delta^{18}O$ values can be seen in the inset in Figure 11, where $\delta^{18}O$ values start at ~5.5‰ and rise until ~13.0‰. Additionally, the granite samples which have negative εHf starting values could represent isotopic ingrowth, meaning that the initial magma was extracted from the mantle at a much earlier time (zircons crystallized at ~3.3 Ga); nearly 800 Ma prior to the time when the granitoids crystallized.

The Bell Creek zircons with ages greater than the emplacement age of the Bell Creek (inherited) are further evidence of assimilation of older material. Nearby Archean provinces include the Minnesota River Valley (MRV). The MRV is composed of granitic gneiss, amphibolitic gneiss, metagabbro and felsic gneisses and range in age from 2.6-3.7 Ga (Cannon and Gair, 1970; Ayuso et al., 2018). East of the MRV lies the Watersmeet Gneiss Dome which contains gneiss as old as 3.56 Ga (Peterman et al., 1980, Ayuso et al., 2018). The 4.2 Ga zircon is the oldest inherited grain found in the Bell Creek granite and could represent some of the oldest assimilated material in the Superior Province, but, again, in-situ outcrops of this rock have yet to be discovered.

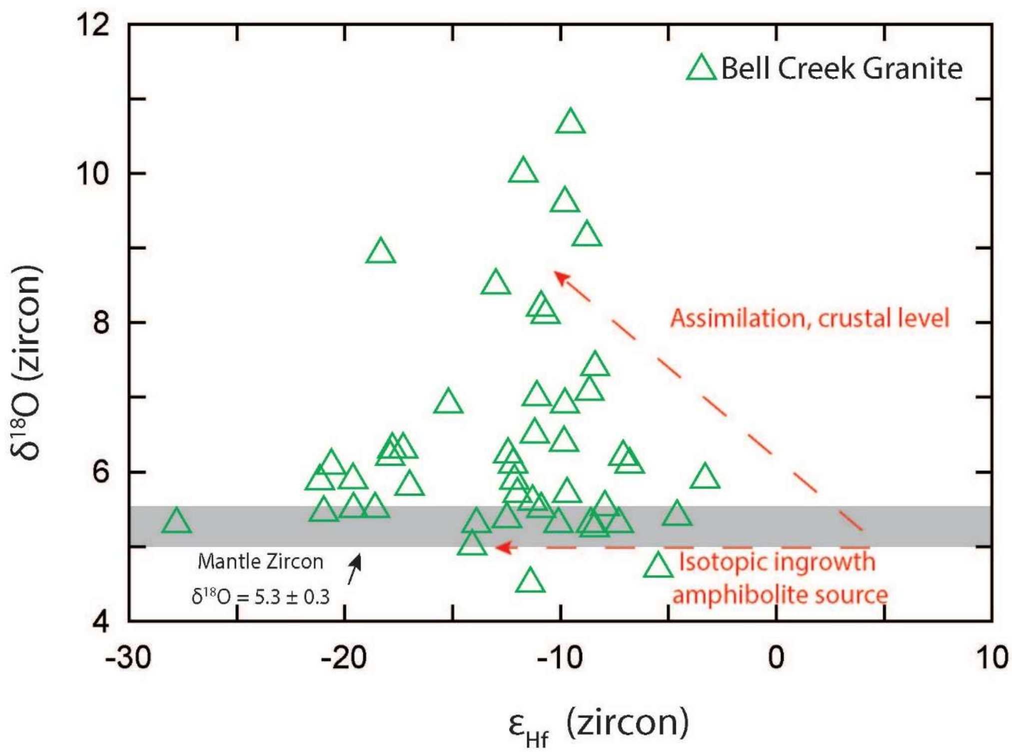


**Figure 12** Plot of εHf versus $\delta^{18}O$ for Bell Creek magmatic zircons. Arrows show direction of isotopic ingrowth of the amphibolite source and assimilation near crustal level. Shaded bar represents the mantle zircon value.

## 5.4 Earth's Crustal Growth

The continental crust contains a record of Earth's geological history and zircons hold the stories of crust-forming events (Hawkesworth et al., 2010; Valley et al., 2005). Nevertheless, there has been constant debate in the geological community on how the continental crust formed and evolved through time (Valley et al, 2005; Hawkesworth et al., 2010; Arndt, 2013; Dhuime et al., 2015).

One of the main components of the Archean crust is the TTG suite, which is mainly comprised of silica-rich rocks that are high in $Na_2O$ (Jahn et al, 1981). These sodic granitoids are present prior to 3.2 Ga, and have been described as being generated by melting of hydrous garnet amphibolite, granulite or eclogite at mantle depths (Smithies et al., 2003; Sizova, 2015). Near the end of the Archean, due to an increase of crustal recycling and continental crust growth, massive intracrustal melting of newly formed TTG crust resulted in the formation of K-rich granitoids (Taylor 1987; Sizova et al., 2015). This time period of continental growth and intracrustal melting resulted in the continental crust becoming enriched in incompatible elements and depleted in Eu, this is also referred to as "cratonization" (Taylor & McLennan, 1995). Near the end of the Archean global heat flow decreased and modern-style plate tectonics began to dominate (Taylor & McLennan, 1995).

The Bell Creek Granitoids have an emplacement age between 2.5 Ga and 2.6 Ga which places them at the end of the Archean during cratonization. Data presented from the Bell Creek granitoids suggests there was more recycling of supracrustal rocks earlier in Earth's history than previously recognized. Valley et al. (2005) identified a trend which showed an increase in $\delta^{18}O$ at the end of the Archean at 2.5 Ga and that $\delta^{18}O$ values maintained a constant rate from about 4.2-2.5 Ga, suggesting that crustal recycling did not begin until <2.5 Ga and juvenile crustal formation dominated prior to that (Figure 13). The Bell Creek data is slightly inconsistent with Valley's trend as it demonstrates higher $\delta^{18}O$ values prior to 2.5 Ga suggesting some crustal recycling occurred >2.5 Ga (Figure 13). However, there is a noticeable increase in higher $\delta^{18}O$ values at 2.5 Ga, suggesting more crustal recycling occurred during this time (Figure 13). The Bell Creek data supports the theory of Earth's crustal recycling increasing at 2.5 Ga, but also provides evidence that recycling could have occurred prior to 2.5 Ga.

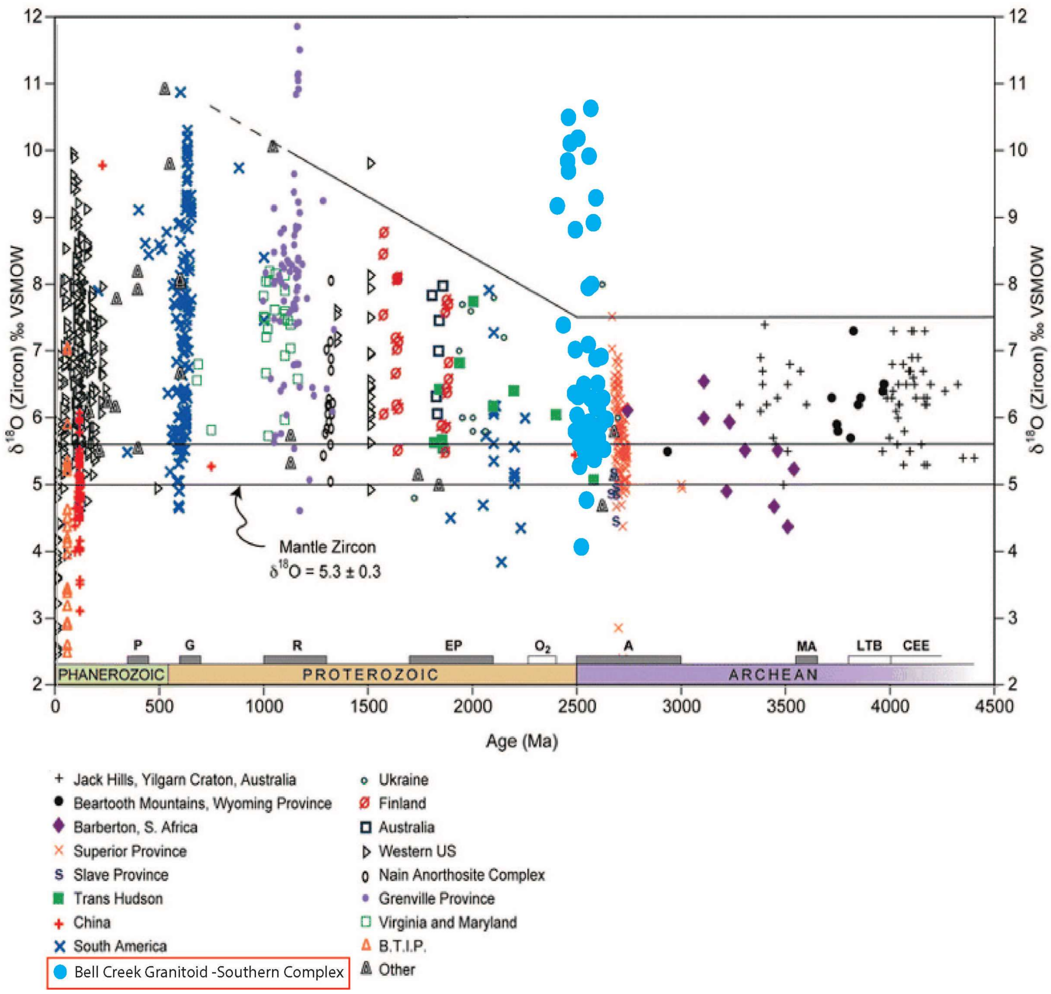


**Figure 13** Compilation of $\delta^{18}O$(zircon) versus age for 1,200 rocks of known age. This plot shows relatively low $\delta^{18}O$ throughout the Archean, which is proceeded by higher $\delta^{18}O$ after 2.5 Ga reflecting recycling of high $\delta^{18}O$ material and maturation of the crust. The Southern Complex can be seen at the end of the Archean when $\delta^{18}O$ begins to rise. The Southern Complex represents a wide range of $\delta^{18}O$ values. Modified from Valley et al. (2005).

# 6 Conclusions

A comprehensive dataset of whole rock major and trace elements and zircon geochemistry for the Bell Creek granitoids give an emplacement age between 2.5-2.6 Ga for the suite. The integration of the O-Hf isotopic data supports the conclusion of Hoffman (1987), that the granitoids were produced by both partial melting of pre-existing lower crustal basement lithologies followed by assimilation of metasedimentary country rock. Therefore, the petrogenesis of the Bell Creek granitoids involved melt contributions from a juvenile mantle source and from the recycling of a supracrustal source, which must have been a pelitic source due to the high-K nature of the granitoids. In addition, a Hf model age of 3.3 Ga suggests the primary protolith was extracted from the mantle at this time. Support for assimilation is also given by U-Pb dates and O-Hf isotopes that indicate inherited zircons ranging from 2.7-4.2 Ga.

A magmatic emplacement age between 2.5-2.6 Ga and high $\delta^{18}O$ values of magmatic zircons from the Bell Creek granitoids imply that Earth was recycling supracrustal material during periods of crustal growth in the Archean. This contrasts the idea proposed by Valley et al. (2005) that throughout the Archean there was a uniformity of mantle-like $\delta^{18}O$ values and a lack of recycling of supracrustal material. The data from the Bell Creek granitoids indicate there was recycling of supracrustal material throughout the Archean. Comprehensive studies of other Archean plutons should be completed to further investigate the history of recycling during the Archean. Results from such studies would shed light on the debate on crustal growth and recycling during the early Earth.

# 7 References

Amelin, Y., Lee, D.-C., Halliday, A. N., & Pidgeon, R. T. (1999). Nature of the Earth's earliest crust from hafnium isotopes in single detrital zircons. Nature, 399 (6733), 252-255. doi:10.1038/20426Arndt, N. T. (2013). The Formation and Evolution of the Continental Crust. Geochemical Perspectives, 2(3), 405-405.

Atherton, M. P. (1993). Granite magmatism. Journal of the Geological Society, 150(6), 1009-1023.

Ayuso, R.A., Schulz, K.J., Cannon, W.F., Woodruff, L.G., Vazquez, J.A., Foley, N.K. , and Jackson, J. New U-Pb Zircon Ages for Rocks from the Granite-Gneiss Terrane in Northern Michigan: Evidence for Events at ~3750, 2750, and 1850 Ma. 64th Institute on Lake Superior Geology Proceedings, v. 64, Part 1, Program and Abstracts, p 7-8.

Belousova, E. A., Kostitsyn, Y. A., Griffin, W. L., Begg, G. C., O'Reilly, S. Y., & Pearson, N. J. (2010). The growth of the continental crust: Constraints from zircon Hf-isotope data. Lithos, 119(3), 457-466.

Brown, M. (1994). The generation, segregation, ascent and emplacement of granite magma: the migmatite-to-crustally-derived granite connection in thickened orogens. Earth-Science Reviews, *36*(1-2), 83-130.

Brown, M. (2007). Crustal melting and melt extraction, ascent and emplacement in orogens: mechanisms and consequences. Journal of the Geological Society, 164(4), 709-730.

Cannon, W. F., and Gair, J. E. (1970) A Revision of Stratigraphic Nomenclature for Middle Precambrian Rocks in Northern Michigan. GSA Bulletin; 81 (9) 2843-2846.

Cannon, W. F., and Simmons, G.C. (1973). Geology of Part of the Southern Complex, Marquette District, Michigan. Journal of Research, US Geological Survey, 1, 165-172.

Cannon, W.F., and Simmons, G.C., 1973, Geology of part of the southern complex, Marquette district, Michigan: U.S. Geological Survey, Journal of Research of the U.S. Geological Survey v.1, no. 2, p. 165-172., scale 1:162,500.

Card, K.D., Ciesielski, A. (1986). DNAG #1. Subdivisions of the Superior Province of the Canadian Shield. Geoscience Canada, 13(1).

Chappell, B. W., & White, A. J. (2001). Two contrasting granite types: 25 years later. Australian Journal of Earth Sciences, 48(4), 489-499.

Chu, M.-F., Chung, S.-L., Song, B., Liu, D., O'Reilly, S. Y., Pearson, N. J., . . . Wen, D.-J. (2006). Zircon U-Pb and Hf isotope constraints on the Mesozoic tectonics and crustal evolution of southern Tibet. Geology, 34(9), 745-748.

Corfu, F. (1988). Differential response of U-Pb systems in coexisting accessory minerals, Winnipeg River Subprovince, Canadian Shield: implications for Archean crustal growth and stabilization. Contributions to Mineralogy and Petrology, *98*(3), 312-325.

Davidson, J., Turner, S., Handley, H., Macpherson, C., & Dosseto, A. (2007). Amphibole "sponge" in arc crust? Geology, 35(9), 787-790.

Dhuime, B., Wuestefeld, A., & Hawkesworth, C. J. (2015). Emergence of modern continental crust about 3 billion years ago. Nature Geoscience, 8, 552.

Finch, R.J., Hanchar, J. M. (2003). Structure and Chemistry of Zircon and Zircon-Group Minerals. Reviews in Mineralogy and Geochemistry, 53, 1-25.

Gair, J. E., Thaden, R. E. (1968). Geology of the Marquette and Sands quadrangles, Marquette County, Michigan. United States Geological Survey Professional Paper 379.

Galli, A., Grassi, D., Sartori, G., Gianola, O., Burg, J. P., & Schmidt, M. W. (2019). Jurassic carbonatite and alkaline magmatism in the Ivrea zone (European Alps) related to the breakup of Pangea. Geology, 47(3).

Guillong M., Quadt A., Sakata S., Peytcheva, I. and Bachmann O. (2014). LA-ICP-MS Pb–U dating of young zircons from the Kos–Nisyros volcanic centre, SE Aegean arc. Royal Society of Chemistry, 29, 963-970.

Goldich, Samuel S. et al. (1961). The Precambrian Geology and Geochronology of Minnesota. Minnesota Geological Survey Bulletin 41. 193.

Grant, J. (1972). Minnesota River Valley, southwestern Minnesota. In Geology of Minnesota; A Centennial Volume. Minnesota Geological Survey, St. Paul, Minnesota. 177-196.

Hawkesworth, C. J., and Kemp, A.I.S. (2006). Using hafnium and oxygen isotopes in zircons to unravel the record of crustal evolution. Chemical Geology, 226(3-4), 144-162.

Hawkesworth, C. J., Dhuime, B., Pietranik, A. B., Cawood, P. A., Kemp, A. I. S., & Storey, C. D. (2010). The generation and evolution of the continental crust. Journal of the Geological Society, 167(2), 229-248.

Hoffman, M. A. (1987). The Southern Complex: Geology, Geochemistry, Mineralogy and Mineral Chemistry of Selected Uranium and Thorium-rich Granites. (PhD), Michigan Technological University.

Kinny, P. D., Maas, R. (2003). Lu–Hf and Sm–Nd isotope systems in zircon. Reviews in Mineralogy and Geochemistry, 53(1), 327-341. Reviews in Mineralogy and Geochemistry.

Kita, N. T. (2009). High precision SIMS oxygen isotope analysis and the effect of sample topography. Chemical Geology, 264(1-4), 43-57.

Kusky, T. M., & Polat, A. (1999). Growth of granite–greenstone terranes at convergent margins, and stabilization of Archean cratons. Tectonophysics, 305(1), 43-73.

Maniar, P. D., & Piccolo, P. M. (1989). Tectonic discrimination of granitoids. GSA Bulletin, 101(5), 635-643. GSA Bulletin.

Matteini, M., et al. (2010). "Combined U-Pb and Lu-Hf isotope analyses by laser ablation MC-ICP-MS: methodology and applications." Anais da Academia Brasileira de Ciências 82(2): 479-491.

McDonough, W.F, and Sun, S.-S. “The Composition of the Earth.” Chemical Geology 120.3 (1995): 223–253. Web.

Middlemost, E. A. K. (1994). Naming materials in the magma/igneous rock system. Earth Science Reviews, 37(3-4), 215-224.

Morey, G., Sims, P., & Morey, G. (1976). Boundary between two Precambrian W terranes in Minnesota and its geologic significance. Bulletin of the Geological Society of America, 87(1), 141–152.

Moyen, J.-F. (2009). High Sr/Y and La/Yb ratios: The meaning of the “adakitic signature”. Lithos, 112(3), 556-574.

Pearce, J. A., Harris, N. B. W., Tindle, A. G. (1984). Trace Element Discrimination Diagrams for the Tectonic Interpretation of Granitic Rocks. Journal of Petrology, 25(4), 956-983.

Pearce, J. A. and I. J. Parkinson (1993). "Trace element models for mantle melting: application to volcanic arc petrogenesis." Geological Society, London, Special Publications 76(1): 373-403.

Peterman, Z., Zartman, R., & Sims, P. K. (1980). Tonalitic gneiss of early Archean age from northern Michigan. Geological Society of America. 182, 125-134.

Roberts, M. P., & Clemens, J. D. (1993). Origin of high-potassium, calc-alkaline, I-type granitoids. Geology, 21(9), 825-828.

Schmus, W. R. V., & Woolsey, L. L. (1975). Rb–Sr Geochronology of the Republic Area, Marquette County, Michigan. Canadian Journal of Earth Sciences, 12(10), 1723-1733.

Schulz, K. J., & Cannon, W. F. (2007). The Penokean orogeny in the Lake Superior region. Precambrian Research, 157(1), 4-25.

Sims, P. K. (1991). Great Lakes Tectonic Zone in Marquette Area, Michigan-Implications for Archean Tectonics in North-Central United States (Vol. United States Geological Society Bulletin 1904-E).

Sizova, E., Gerya, T., Stüwe, K., & Brown, M. (2015). Generation of felsic crust in the Archean: a geodynamic modeling perspective. Precambrian Research, 271, 198-224.

Smithies, R. H., Champion, D. C., & Cassidy, K. F. (2003). Formation of Earth's early Archaean continental crust. Precambrian Research, 127(1-3), 89-101.

Sun, S., & McDonough, W. F. (1989). Chemical and isotopic systematics of oceanic basalts: implications for mantle composition and processes. 42(1), 313-345. Geological Society, London, Special Publications

Sylvester, Paul J. "Archean granite plutons." Developments in Precambrian geology. Vol. 11. Elsevier, 1994. 261-314.

Taylor, S. R. (1987). "Geochemical and Petrological Significance of the Archaean-Proterozoic Boundary." Geological Society, London, Special Publications 33(1): 3-8.

Taylor, S. R. and S. M. McLennan (1985). "The continental crust: its composition and evolution."

Taylor, S. R. and S. M. McLennan (1995). "The geochemical evolution of the continental crust." Reviews of Geophysics 33(2): 241-265.

Tinkham, D. K. (1997). Tectonic Evolution of the Southern Complex Regiong of the Penokean Orogenic Belt, Upper Peninsula Michigan: The Formation of Precambrian Dome-and-Keel Architecture (MS), University of Illinois.

Trow, J. (1979). Diamond drilling for geologic information in the middle Precambrian basins in the western portion of northern Michigan. Final report (No. GJBX-162 (79)). Michigan Dept. of Natural Resources, Lansing (USA). Geological Survey Division.

Valley, J. W. (2003). Oxygen Isotopes in Zircon. Reviews in Mineralogy and Geochemistry, 53(1), 343-385. Reviews in Mineralogy and Geochemistry.

Valley, J. W., Lackey, J. S., Cavosie, A. J., Clechenko, C. C., Spicuzza, M. J., Basei, M. A. S. (2005). 4.4 billion years of crustal maturation: oxygen isotope ratios of magmatic zircon. Contrib Mineral Petrol. 150(6).

Vallini, D. A., Cannon, W. F., & Schulz, K. J. (2006). Age constraints for Paleoproterozoic glaciation in the Lake Superior Region: detrital zircon and hydrothermal xenotime ages for the Chocolay Group, Marquette Range Supergroup. *Canadian Journal of Earth Sciences*, *43*(5), 571-591.

Vervoort, J. D., & Blichert-Toft, J. (1999). Evolution of the depleted mantle: Hf isotope evidence from juvenile rocks through time. Geochimica et Cosmochimica Acta, 63(3), 533-556.

Vervoort, J. (2015). "Lu-Hf dating: the Lu-Hf isotope system." Encyclopedia of Scientific Dating Methods: 379-390.

Vijaya Kumar, K., Ernst, W. G., Leelanandam, C., Wooden, J. L., Grove, M. J. (2011). Origin of ~2.5 Ga potassic granite from the Nellore Schist Belt, SE India: textural,

Whalen, J. B., Currie, K. L., Chappell, B. W. J. C. t. M., & Petrology. (1987). A-type granites: geochemical characteristics, discrimination and petrogenesis. Contrib Mineral Petrol. 95(4), 407-419.

Wilkin, R. T., & Bornhorst, T. J. (1992). Geology and geochemistry of granitoid rocks in the Archean Northern complex, Michigan, U.S.A. Canadian Journal of Earth Sciences, 29(8), 1674-1685.

Zeh, A., Stern, R. A., & Gerdes, A. (2014). The oldest zircons of Africa—Their U–Pb–Hf–O isotope and trace element systematics, and implications for Hadean to Archean crust–mantle evolution. Precambrian Research, 241, 203-230.

# A Copyright documentation

Figure 12: "4.4 billion years of crustal maturation: oxygen isotope ratios of magmatic zircon" by Valley, J.W., Lackey, J.S., Cavosie, A.J. et al. at Contributions to Mineralogy and Petrology. Licensed under 4615400368135 via Springer Nature. Accessed June 2019.